On the Mechanism of the Initiation Reaction in Grubbs-Hoveyda Complexes

Vasco Thiel, Marina Hendann, Klaus-Jürgen Wannowius, Herbert Plenio*

Organometallic Chemistry, FB Chemie, Petersenstr. 18, 64287 Darmstadt, Germany, e-mail: plenio@tu-darmstadt.de

Supporting Information

General Procedures

All reactions were conducted in oven-dried glassware. Reactions were performed in Schlenk flasks under a positive pressure of argon or nitrogen. The flasks were fitted with rubber septa and gas-tight syringes with stainless steel needles or double-cannulae were used to transfer air- and moisture-sensitive liquids. Column chromatography was carried out with granular silica (63–200 μm). Thin layer chromatography (TLC) was performed using alumina plates pre-coated with 0.2 mm 63–200 mesh silica impregnated with a fluorescent indicator (254 nm). TLC plates were visualized by exposure to UV light (254 nm) or stained with either iodine vapor or an aqueous solution of potassium permanganate.

Materials

Commercial reagents and solvents were used as received with the following exceptions: toluene, dichloromethane, pentane, and diethyl ether were degassed and subsequently dried by passing through Al_2O_3 and/or by storing over molecular sieves. Tetrahydrofuran was dried over sodium/benzophenone and distilled onto molecular sieves. C_6D_6, $CDCl_3$, and toluene-d_8 were dried over molecular sieves and degassed by applying three cycles of freeze-pump-thaw technique. Styrene, n-butyl vinyl ether, 1-hexene, and neohexene were condensed prior to use to remove containing stabilizers or polymerized material and kept under argon. The following compounds were synthesized according to literature procedures: diethyl diallyl malonate,[1] **1(H, F, NO_2, NEt_2, OiPr)**,[2,3,4] **2(Me, F, NO_2, NEt_2, OiPr)**,[2,3,4] **3(H)**,[5] 2-isopropoxy-5-aminostyrene[6] and 2-bromo-5-nitrophenol[7].

Instrumentation

Proton nuclear magnetic resonance (^{1}H NMR) spectra were recorded with Bruker DRX300 and Bruker DRX500 spectrometers, are reported in parts per million on the δ scale, and are referenced from the residual protium in the NMR solvent ($CDCl_3$: δ 7.26 [$CHCl_3$], C_6D_6: δ 7.16 [C_6D_5H], DMSO-d_6: δ 2.50 [DMSO-d_5]) or from Me_4Si (0 ppm). Data are reported as follows: chemical shift [multiplicity (s = singlet, d = doublet, t = triplet, q = quartet, hept = heptet, m = multiplet), coupling constant(s) (J) in Hertz, integration, assignment]. ^{13}Carbon nuclear magnetic resonance spectra were recorded with a Bruker DRX300 and Bruker DRX500 spectrometers, are reported in parts per million on the δ scale, and are referenced from the carbon

resonances of the solvent ($CDCl_3$: δ 77.16, C_6D_6: δ 128.06, DMSO-d_6: δ 39.52) or from Me_4Si (0 ppm). Data are reported as follows: chemical shift. Mass spectra were recorded on a Finnigan MAT95 spectrometer using electron ionization (EI). UV-Vis spectrophotometric data were acquired on a Analytik Jena SPECORD S 600 UV-Vis spectrophotometer. Cyclic voltammetry was performed using a standard electrochemical instrumentation consisted of an EG&G 273A-2 potentiostat-galvanostat. A three-electrode configuration was employed. The working electrode was a Pt disk (diameter 1 mm) sealed in soft glass with a Pt wire as a counter electrode. The pseudo reference electrode was a Ag wire. Potentials were calibrated internally against the formal potential of octamethylferrocene (-0.1 V vs. Ag/AgCl). All cyclic voltammograms were recorded in dry CH_2Cl_2 under an atmosphere of argon, supporting electrolyte NBu_4PF_6 (c = 0.1 mol/L).

Synthesis of ruthenium complexes and precursors

2- Isopropoxy-5-diethylaminostyrene S1

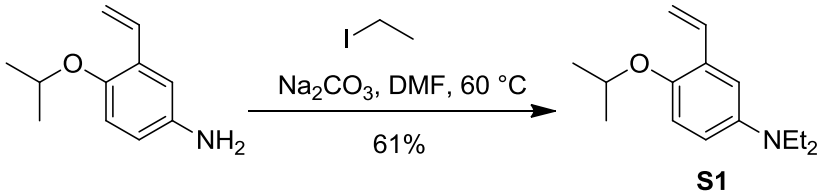

S1

Ethyl iodide (195 µL, 2.5 mmol, 2.5 equiv) was added to a suspension of 2-isopropoxy-5-aminostyrene (173 mg, 1.0 mmol, 1.0 equiv) and sodium carbonate (318 mg, 3.0 mmol, 3.0 equiv) in dimethylformamide (5 mL) at 60 °C. After 24 h of stirring at 60 °C, the reaction mixture was diluted with water (5 mL) and extracted with ethyl acetate (3 × 10 mL). The combined organic layers were washed with saturated sodium chloride solution (1 × 10 mL), dried over anhydrous magnesium sulfate, filtered and concentrated under reduced pressure. The resulting oil was purified by column chromatography on silica (eluent: ethyl acetate/cyclohexane = 1/20) to afford 2-isopropoxy-5-diethylaminostyrene **S1** (138 mg, 61%) as an orange oil.

^{1}H NMR (500 MHz, $CDCl_3$): δ 7.05 (dd, J = 17.8, 11.1 Hz, 1H, Ar−C**H**−CH_2), 6.87 (d, J = 2.5 Hz, 1H, Ar−**H**), 6.81 (d, J = 8.9 Hz, 1H, Ar−**H**), 6.64 (dd, J = 8.8, 2.6 Hz, 1H, Ar−**H**), 5.69 (dd, J = 17.8, 1.5 Hz, 1H, Ar−CH−C**H**$_2$), 5.21 (dd, J = 11.1, 1.4 Hz, 1H, Ar−CH−C**H**$_2$), 4.32 (hept, J = 6.1 Hz, 1H, O−C**H**−$(CH_3)_2$), 3.29 (q, J = 7.1 Hz, 4H, N−(C**H**$_2$−$CH_3)_2$), 1.31 (d, J = 6.1 Hz, 6H, O−CH−(C**H**$_3)_2$), 1.13 (t, J = 7.1 Hz, 6H, N−(CH_2-−C**H**$_3)_2$).

^{13}C NMR (126 MHz, $CDCl_3$): δ 147.4, 143.3, 132.9, 129.3, 117.9, 114.8, 113.5, 111.7, 72.7, 45.3, 22.5, 12.7.

TLC (ethyl acetate/cyclohexane = 1/20), R*f*: 0.67 (UV).

Synthesis of 2(NEt_2)

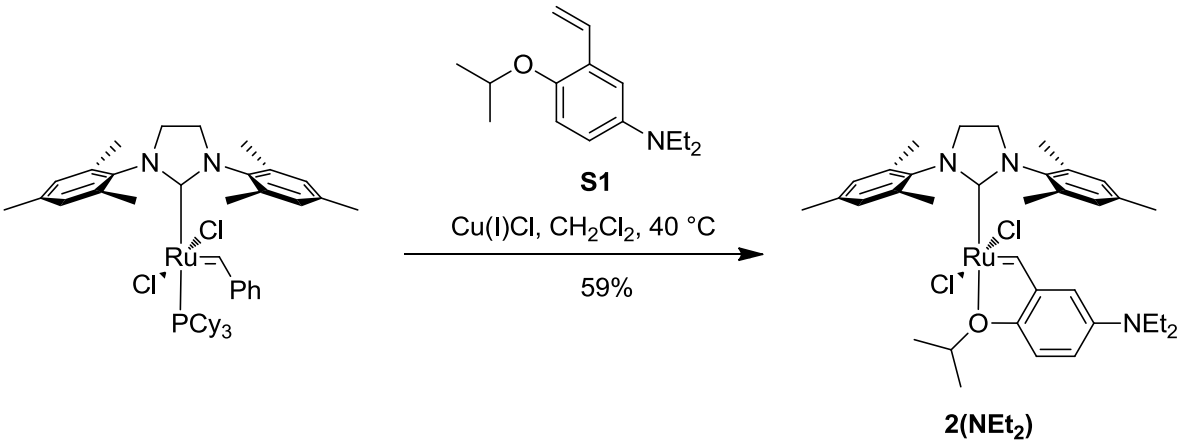

A solution of 2-isopropoxy-5-diethylaminostyrene **S1** (94 mg, 0.40 mmol, 1.3 equiv) in dichloromethane (5 mL) was added to a suspension of Grubbs II catalyst (200 mg, 0.31 mmol, 1.0 equiv) and copper(I) chloride (123 mg, 1.24 mmol, 4 equiv) in dichloromethane (20 mL) at 40 °C under Schlenk conditions. After 1h stirring at 40 °C, evaporation of the solvent following column chromatography on silica (eluent: ethyl acetate/cyclohexane = 1/5) afforded the Grubbs-Hoveyda complex **2(NEt_2)** (128 mg, 59%) as a greenish-brown microcrystalline solid.

^{1}H NMR (500 MHz, $CDCl_3$): δ 16.35 (s, 1H, Ru=C**H**), 7.06 (s, 4H, Mes−**H**), 6.87 (dd, J = 8.8, 2.4 Hz, 1H, Ar−**H**), 6.47 (d, J = 2.4 Hz, 1H, Ar−**H**), 6.63 (d, J = 8.8 Hz, 1H, Ar−**H**), 4.78 (hept, J = 6.0 Hz, 1H, O−C**H**−$(CH_3)_2$), 4.18 (s, 4H, N−C**H**$_2$−C**H**$_2$−N), 3.23 (q, J = 7.0 Hz, 4H, N−(C**H**$_2$−$CH_3)_2$), 2.48 (s, 12H, Mes−C**H**$_3$), 2.39 (s, 6H, Mes−C**H**$_3$), 1.23 (d, J = 6.0 Hz, 6H, O−CH−(C**H**$_3)_2$), 1.08 (t, J = 7.0 Hz, 6H, N−(CH_2−C**H**$_3)_2$).

^{13}C NMR (126 MHz, $CDCl_3$): δ 299.0, 212.7, 145.8, 144.3, 143.9, 139.6, 139.4, 138.7, 129.4, 114.6, 113.2, 108.0, 74.2, 51.6, 45.4, 31.2, 27.1, 21.3, 12.8.

HR-MS (EI), m/z: 697.21905 [M^+] calcd. 697.2131 (Δ = 5.9 mmu).

TLC (ethyl acetate/cyclohexane = 1/5), R*f*: 0.31 (greenish-brown spot).

2-Bromo-5-nitroanisole S2

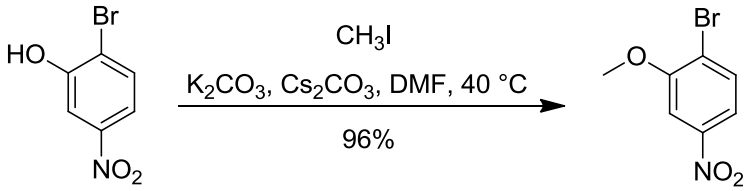

S2

2-Bromo-5-nitrophenol (2.00 g, 9.17 mmol, 1 equiv) was added to a suspension of potassium carbonate (2.60 g, 18.35 mmol, 2 equiv) and cesium carbonate (474 mg, 1.84 mmol, 0.2 equiv) in dimethylformamide (25 mL) at 40 °C. After 10 min, methyl iodide (1.15 mL, 18.35 mmol, 2 equiv) was added and stirring was continued for 48 h at 40 °C. Water (25 mL) was introduced to the flask and the resulting mixture was extracted with ethyl acetate (3 × 20 mL). The combined organic layers were washed with saturated sodium chloride solution (1 × 20 mL), dried over anhydrous magnesium sulfate, filtered and concentrated under reduced pressure. Recrystallization from cyclohexane–acetone (3/1) yielded 2-bromo-5-nitroanisole **S2** (2.05 g, 96%) as colorless crystals.

^{1}H NMR (500 MHz, $CDCl_3$): δ 7.76 – 7.69 (m, 3H, Ar−**H**), 4.00 (s, 3H, O−C**H**$_3$).

^{13}C NMR (126 MHz, $CDCl_3$): δ 156.6, 148.3, 133.8, 119.8, 116.7, 106.6, 56.9.

2-Methoxy-4-nitrostyrene S3

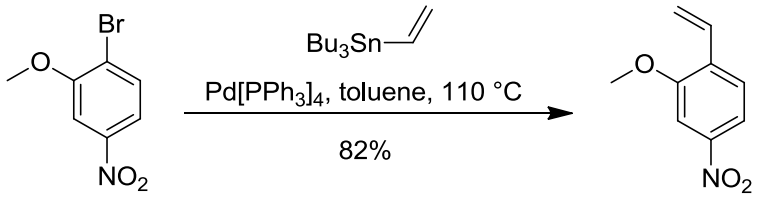

S2 **S3**

A 25-mL Schlenk tube was charged with 2-bromo-5-nitroanisole **S2** (203 mg, 0.88 mmol, 1 equiv) and tetrakis(triphenylphosphine)palladium(0) (51 mg, 0.04 mmol, 5 mol%) under argon. A dry and degassed (3 cycles of freeze-pump-thaw) solution of tributyl(vinyl)tin (281 µL, 0.96 mmol, 1.1 equiv) in toluene (5 mL) was introduced to the reaction vessel and the initial solution was warmed to 110 °C. After stirring for 6h, the dark brown suspension was allowed to cool to RT and concentrated under reduced pressure. A solution of potassium fluoride (0.3 g) in methanol (5 ml) was added. After 1h stirring at RT, the turbid brown solution was diluted with ethyl acetate (5 mL) and washed with water (2 × 10 mL). The resulting aqueous layer was extracted with ethyl acetate (3 × 10 mL) and the combined organic layers were dried over anhydrous magnesium sulfate, filtered and concentrated under reduced pressure. The viscous residue was purified by column chromatography on silica (eluent: ethyl acetate/cyclohexane = 1/10) to afford 2-methoxy-4-nitrostyrene **S3** (128 mg, 82%) as a yellow oil.

^{1}H NMR (300 MHz, $CDCl_3$): δ 7.83 (dd, J = 8.5, 2.2 Hz, 1H, Ar−**H**), 7.72 (d, J = 2.2 Hz, 1H, Ar−**H**), 7.58 (d, J = 8.5 Hz, 1H, Ar−**H**), 7.05 (dd, J = 17.8, 11.2 Hz, 1H, Ar−C**H**−CH_2), 5.90 (dd, J = 17.8, 1.1 Hz, 1H, Ar−CH−C**H**$_2$), 5.48 (dd, J = 11.2, 1.1 Hz, 1H, Ar−CH−C**H**$_2$), 3.95 (s, 3H, O−C**H**$_3$).

^{13}C NMR (75 MHz, $CDCl_3$): δ 157.0, 148.2, 133.5, 130.4, 126.8, 118.8, 116.15, 106.1, 55.2.

TLC (ethyl acetate/cyclohexane = 1/10), R*f*: 0.47 (UV).

Synthesis of 3(NO_2)

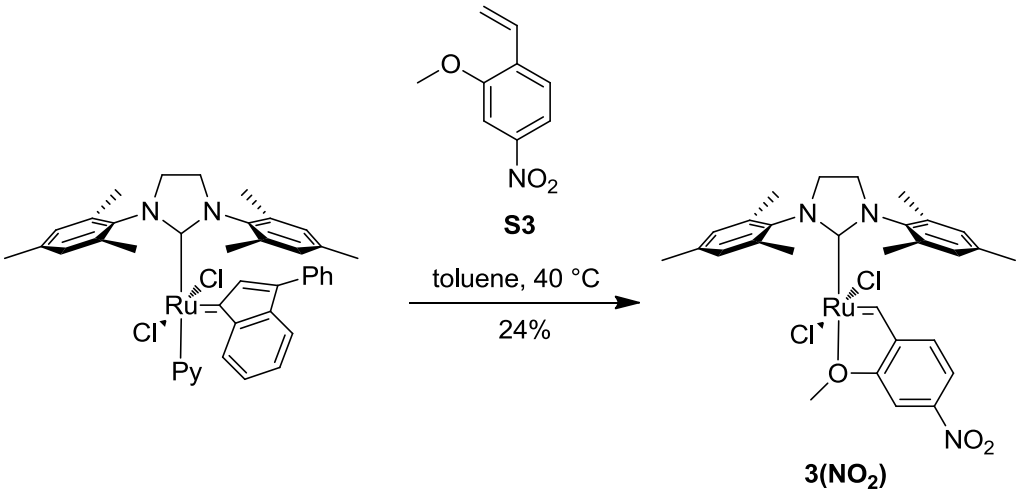

Under Schlenk conditions [dichloro-(3-phenyl-1*H*-inden-1-ylidene)-(1,3-dimesityl-4,5-dihydro-imidazol-2-ylidene)-(pyridine)-ruthenium(II) (250 mg, 0.33 mmol, 1 equiv) was dissolved in toluene (10 mL) and a solution of 2-methoxy-4-nitrostyrene **S3** (53 mg, 0.30 mmol, 0.9 equiv) in toluene (10 mL) was added. Using more of the 2-methoxy-4-nitrostyrene **S3** resulted in the formation of a significant amount of the respective stilbene via cross metathesis. The reaction mixture was stirred for 30 min (longer reaction times resulted in significant decomposition of the product) at 30 °C. Concentration under reduced pressure afforded a dark viscous material which was purified by short column chromatography on silica (ethyl acetate/cyclohexane = 1/2). After washing with pentane (3 × 5 mL) the Grubbs-Hoveyda complex **3(NO_2)** (51 mg, 24%) was obtained as a green-yellowish microcrystalline solid. The complex still contains a small amount (< 5%) of the stilbene, which could not be removed. Attempted careful chromatographic purification resulted in the decomposition of **3(NO_2)**.

^{1}H NMR (500 MHz, $CDCl_3$): δ 16.57 (s, 1H, Ru=C**H**), 7.83 (dd, J = 8.3, 1.9 Hz, 1H, Ar−**H**), 7.77 (s, 1H, Ar−**H**), 7.09 (s, 4H, Mes−**H**) 7.05 (d, J = 8.3 Hz, 1H, Ar−**H**), 4.17 (s, 4H, N−C**H**$_2$−C**H**$_2$−N), 3.94 (s, 3H, O−C**H**$_3$), 2.45 (s, 12H, Mes−C**H**$_3$), 2.43 (s, 6H, Mes−C**H**$_3$).

^{13}C NMR (126 MHz, C_6D_6): δ 282.4, 206.8, 153.2, 146.9, 145.6, 139.3, 138.7, 136.0, 129.8, 121.1, 120.4, 107.3, 59.4, 51.9, 21.3, 19.3.

MS (EI), m/z (%): 644 [$M^{\bullet+}$] corresponds to calculated isotope pattern.

TLC (ethyl acetate/cyclohexane = 1/2), R*f*: 0.24 (green-yellowish spot).

NMR spectra

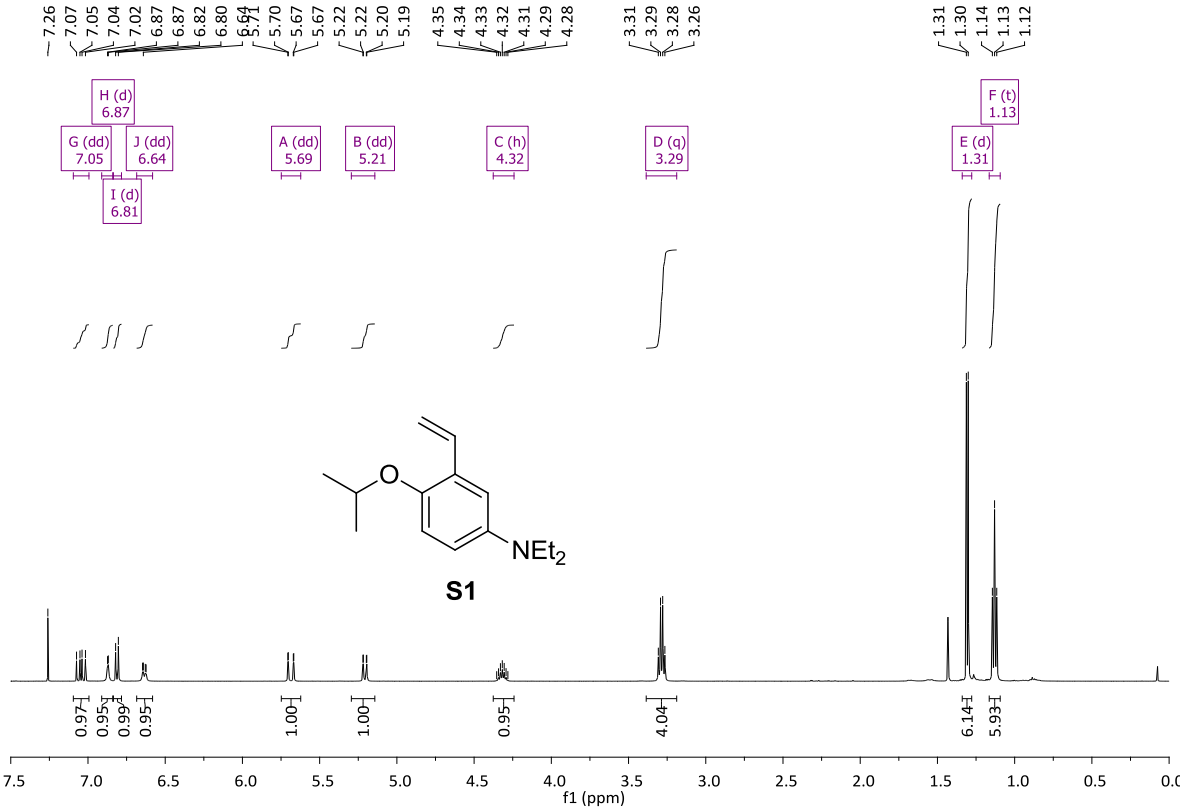

Figure SI-1. ^{1}H NMR spectrum of **S1**.

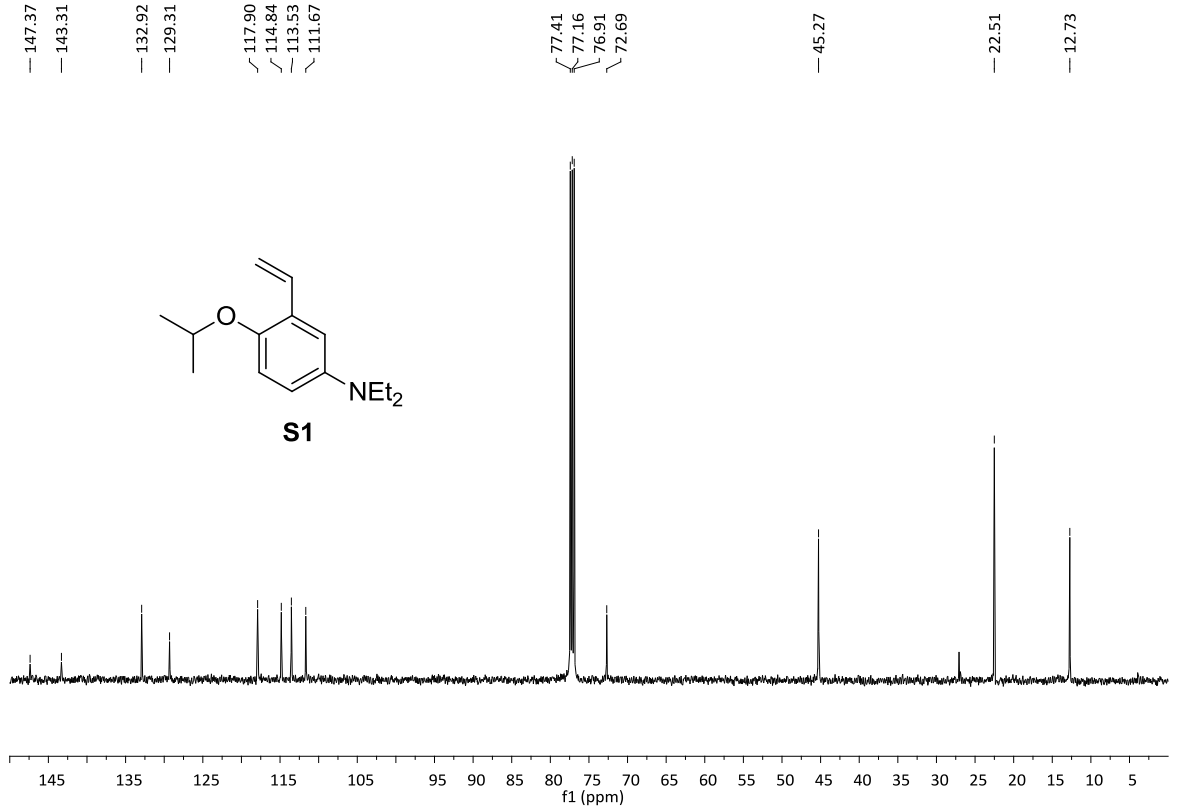

Figure SI-2. ^{13}C NMR spectrum of **S1**.

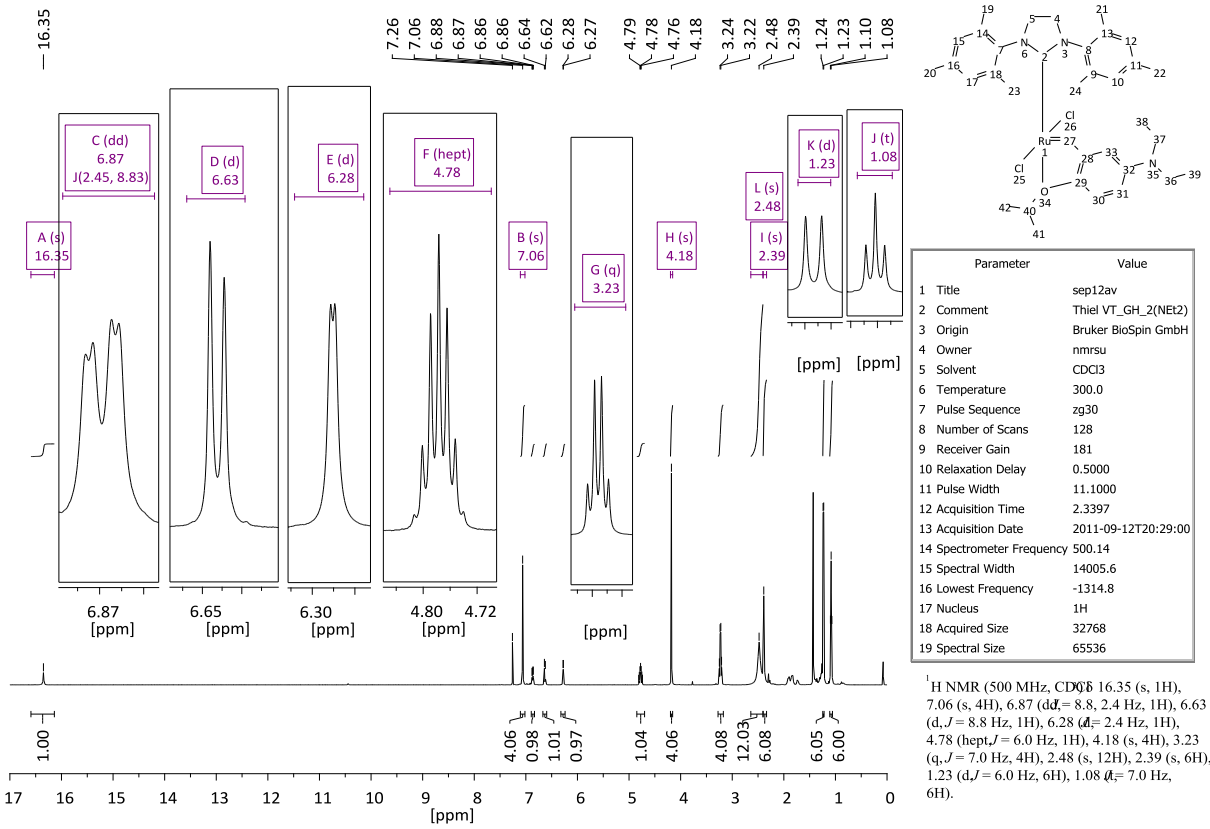

	Parameter	Value
1	Title	sep12av
2	Comment	Thiel VT_GH_2(NEt2)
3	Origin	Bruker BioSpin GmbH
4	Owner	nmrsu
5	Solvent	CDCl3
6	Temperature	300.0
7	Pulse Sequence	zg30
8	Number of Scans	128
9	Receiver Gain	181
10	Relaxation Delay	0.5000
11	Pulse Width	11.1000
12	Acquisition Time	2.3397
13	Acquisition Date	2011-09-12T20:29:00
14	Spectrometer Frequency	500.14
15	Spectral Width	14005.6
16	Lowest Frequency	-1314.8
17	Nucleus	1H
18	Acquired Size	32768
19	Spectral Size	65536

^{1}H NMR (500 MHz, CDCl$_3$) δ 16.35 (s, 1H), 7.06 (s, 4H), 6.87 (dd, J = 8.8, 2.4 Hz, 1H), 6.63 (d, J = 8.8 Hz, 1H), 6.28 (d, J = 2.4 Hz, 1H), 4.78 (hept, J = 6.0 Hz, 1H), 4.18 (s, 4H), 3.23 (q, J = 7.0 Hz, 4H), 2.48 (s, 12H), 2.39 (s, 6H), 1.23 (d, J = 6.0 Hz, 6H), 1.08 (t, J = 7.0 Hz, 6H).

Figure SI-3. ^{1}H NMR spectrum of **2(NEt$_2$)**.

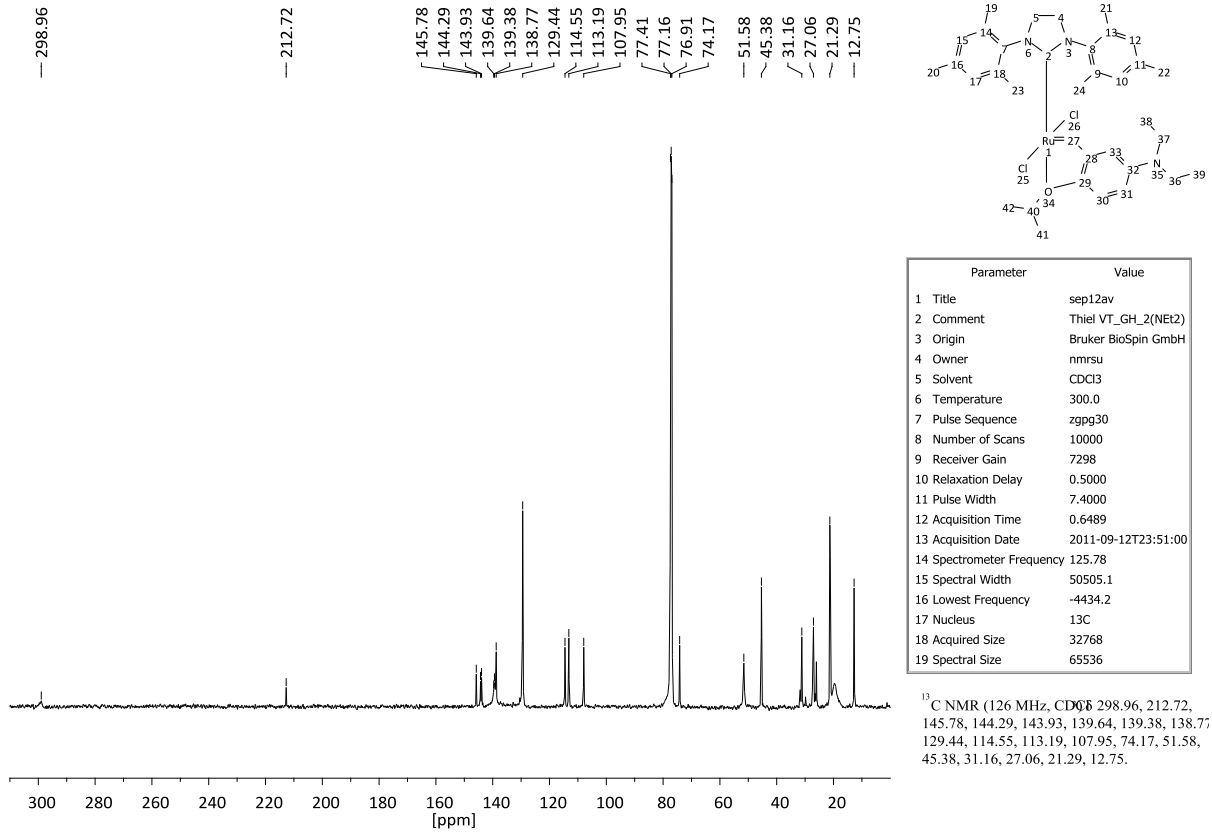

	Parameter	Value
1	Title	sep12av
2	Comment	Thiel VT_GH_2(NEt2)
3	Origin	Bruker BioSpin GmbH
4	Owner	nmrsu
5	Solvent	CDCl3
6	Temperature	300.0
7	Pulse Sequence	zgpg30
8	Number of Scans	10000
9	Receiver Gain	7298
10	Relaxation Delay	0.5000
11	Pulse Width	7.4000
12	Acquisition Time	0.6489
13	Acquisition Date	2011-09-12T23:51:00
14	Spectrometer Frequency	125.78
15	Spectral Width	50505.1
16	Lowest Frequency	-4434.2
17	Nucleus	13C
18	Acquired Size	32768
19	Spectral Size	65536

^{13}C NMR (126 MHz, CDCl$_3$) δ 298.96, 212.72, 145.78, 144.29, 143.93, 139.64, 139.38, 138.77, 129.44, 114.55, 113.19, 107.95, 74.17, 51.58, 45.38, 31.16, 27.06, 21.29, 12.75.

Figure SI-4. ^{13}C NMR spectrum of **2(NEt$_2$)**.

Figure SI-5. ^{1}H NMR spectrum of **S2**.

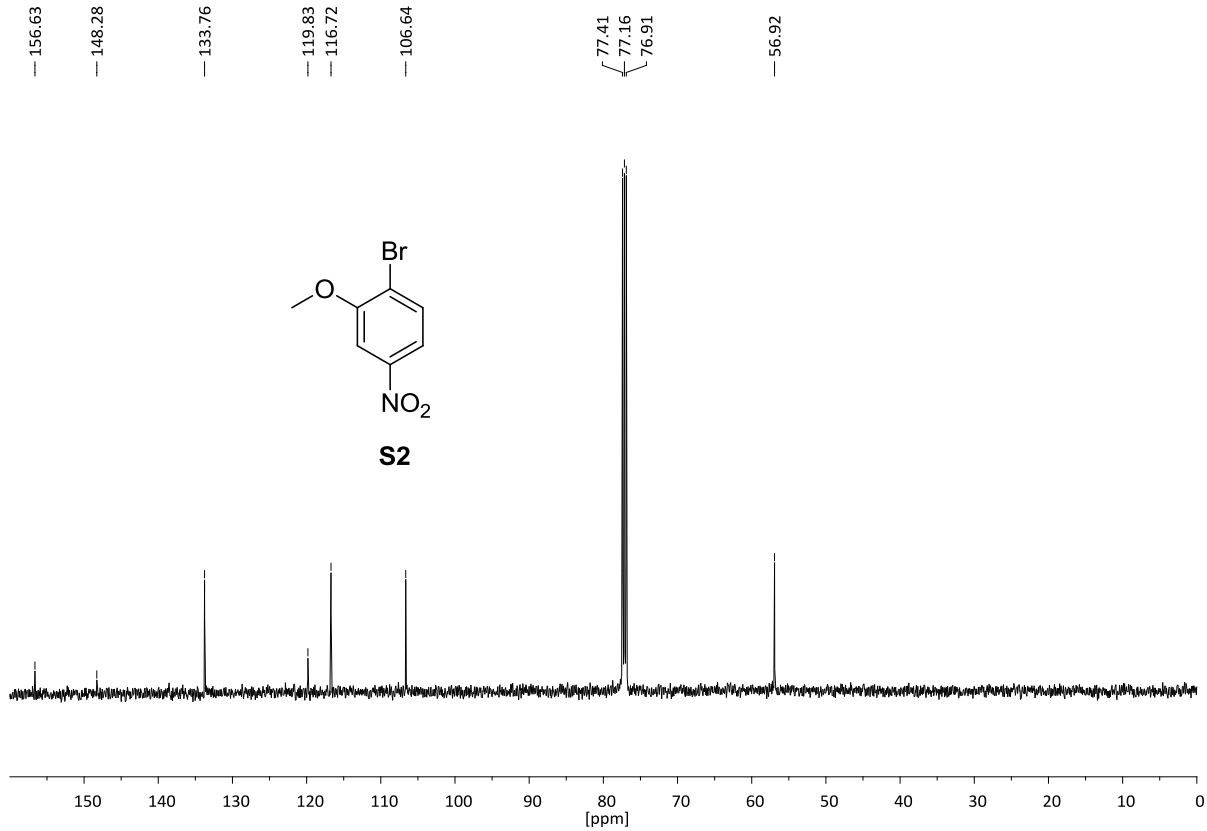

Figure SI-6. ^{13}C NMR spectrum of **S2**.

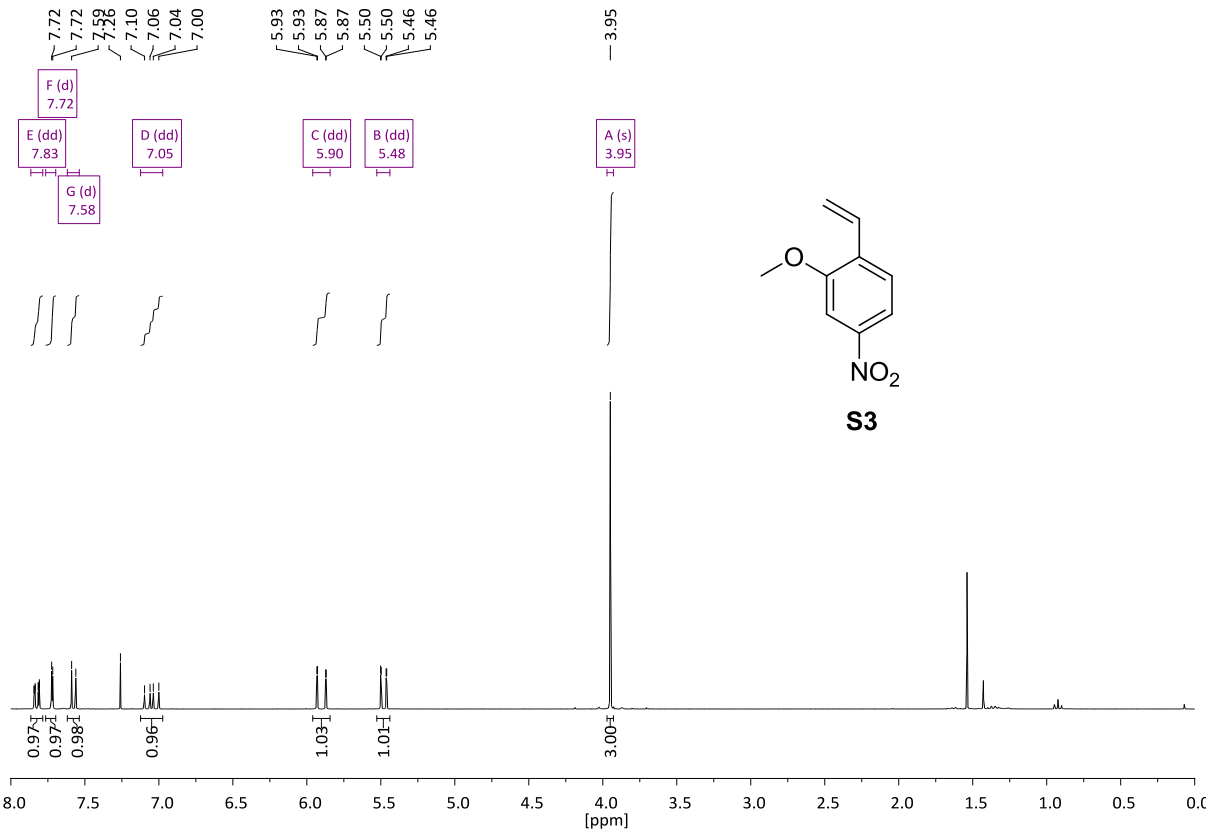

Figure SI-7. ^{1}H NMR spectrum of **S3**.

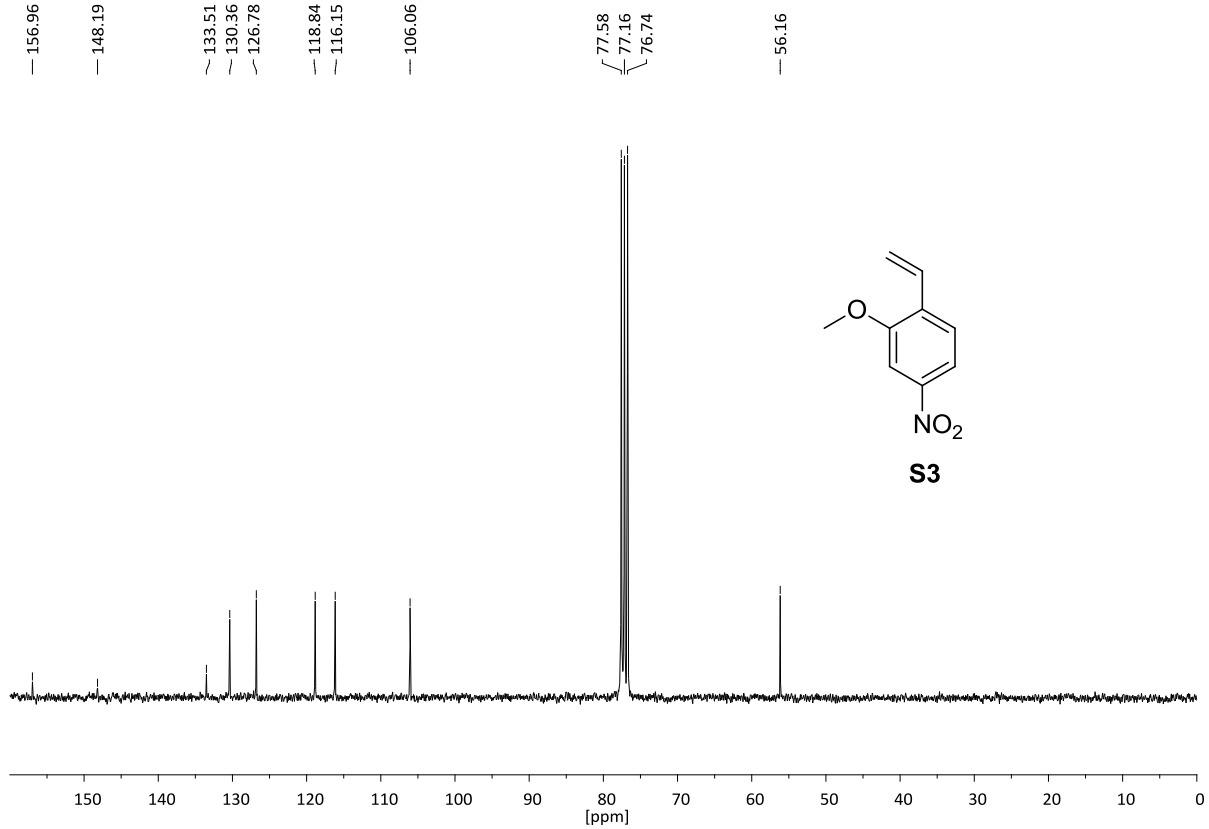

Figure SI-8. ^{13}C NMR spectrum of **S3**.

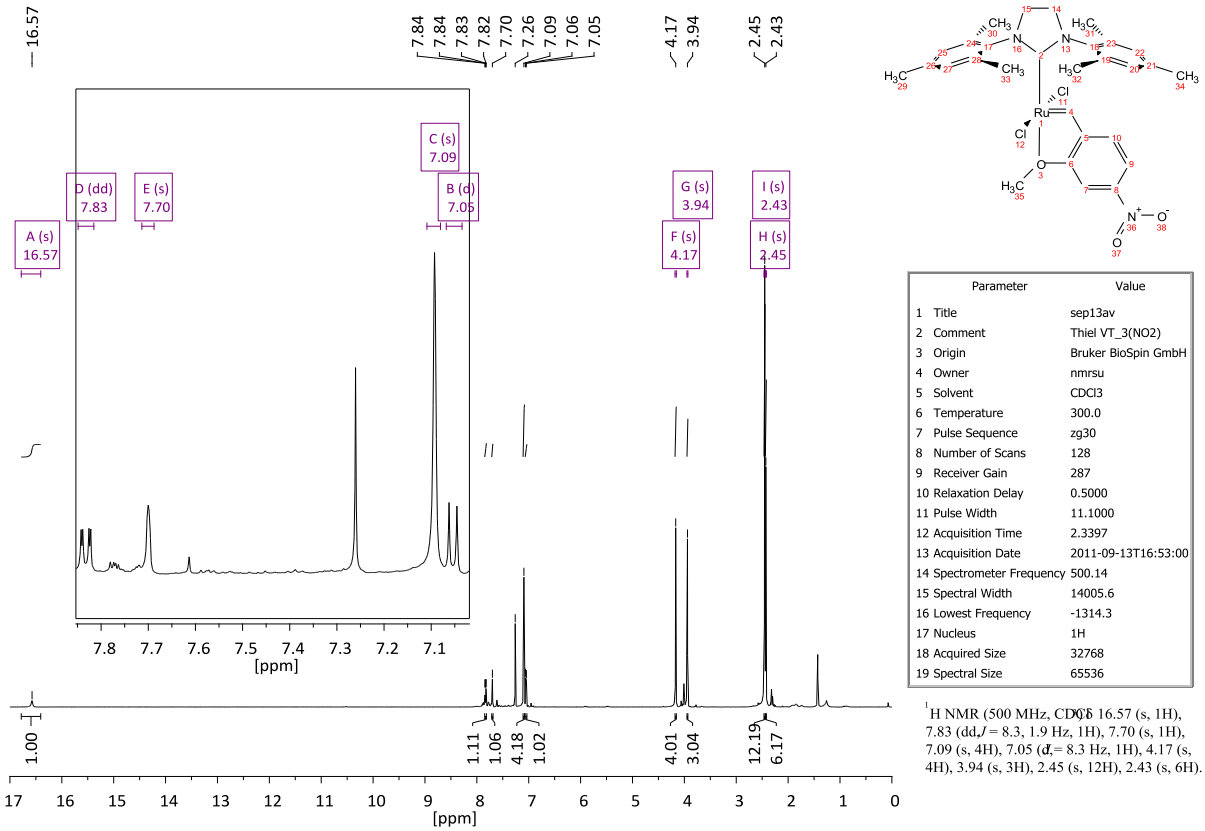

	Parameter	Value
1	Title	sep13av
2	Comment	Thiel VT_3(NO2)
3	Origin	Bruker BioSpin GmbH
4	Owner	nmrsu
5	Solvent	CDCl3
6	Temperature	300.0
7	Pulse Sequence	zg30
8	Number of Scans	128
9	Receiver Gain	287
10	Relaxation Delay	0.5000
11	Pulse Width	11.1000
12	Acquisition Time	2.3397
13	Acquisition Date	2011-09-13T16:53:00
14	Spectrometer Frequency	500.14
15	Spectral Width	14005.6
16	Lowest Frequency	-1314.3
17	Nucleus	1H
18	Acquired Size	32768
19	Spectral Size	65536

^{1}H NMR (500 MHz, $CDCl_3$) δ 16.57 (s, 1H), 7.83 (dd, J = 8.3, 1.9 Hz, 1H), 7.70 (s, 1H), 7.09 (s, 4H), 7.05 (d, J = 8.3 Hz, 1H), 4.17 (s, 4H), 3.94 (s, 3H), 2.45 (s, 12H), 2.43 (s, 6H).

Figure SI-9. ^{1}H NMR spectrum of **3(NO$_2$)**.

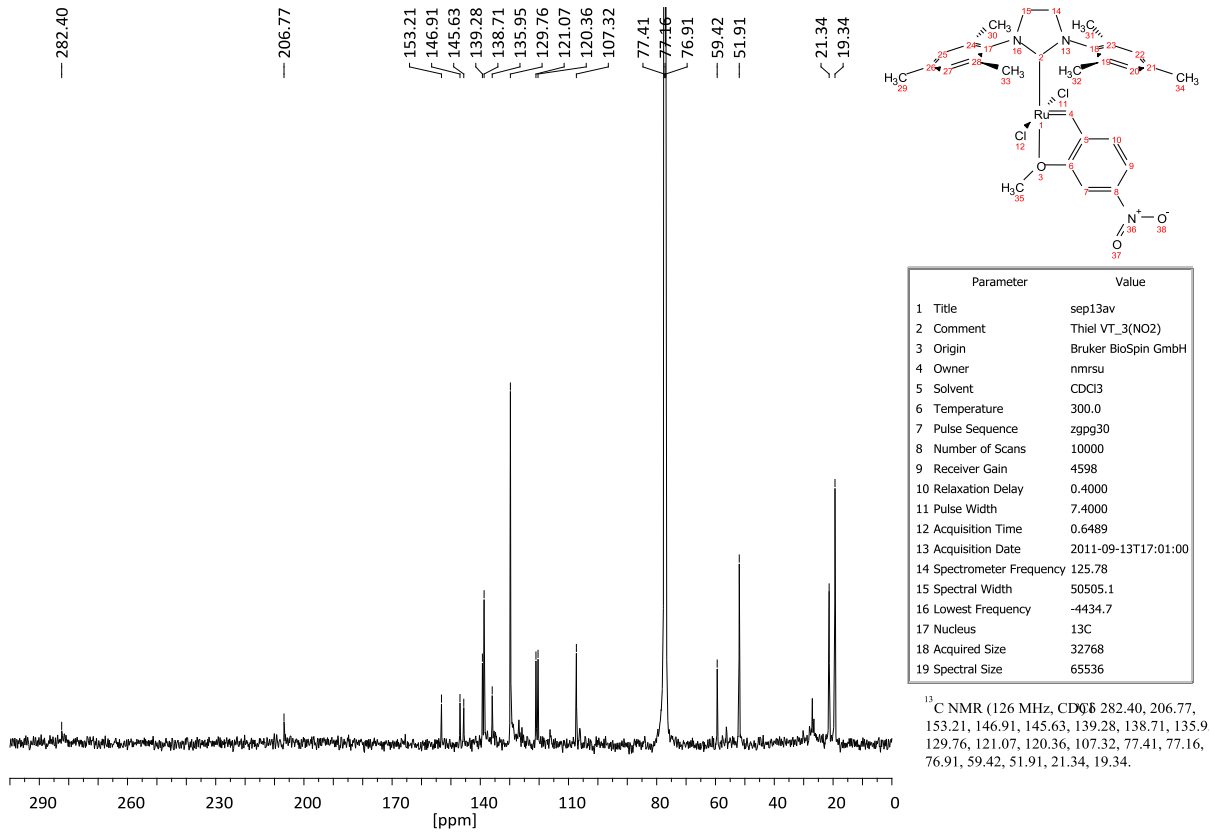

	Parameter	Value
1	Title	sep13av
2	Comment	Thiel VT_3(NO2)
3	Origin	Bruker BioSpin GmbH
4	Owner	nmrsu
5	Solvent	CDCl3
6	Temperature	300.0
7	Pulse Sequence	zgpg30
8	Number of Scans	10000
9	Receiver Gain	4598
10	Relaxation Delay	0.4000
11	Pulse Width	7.4000
12	Acquisition Time	0.6489
13	Acquisition Date	2011-09-13T17:01:00
14	Spectrometer Frequency	125.78
15	Spectral Width	50505.1
16	Lowest Frequency	-4434.7
17	Nucleus	13C
18	Acquired Size	32768
19	Spectral Size	65536

^{13}C NMR (126 MHz, $CDCl_3$) δ 282.40, 206.77, 153.21, 146.91, 145.63, 139.28, 138.71, 135.95, 129.76, 121.07, 120.36, 107.32, 77.41, 77.16, 76.91, 59.42, 51.91, 21.34, 19.34.

Figure SI-10. ^{13}C NMR spectrum of **3(NO$_2$)**.

Mass spectra

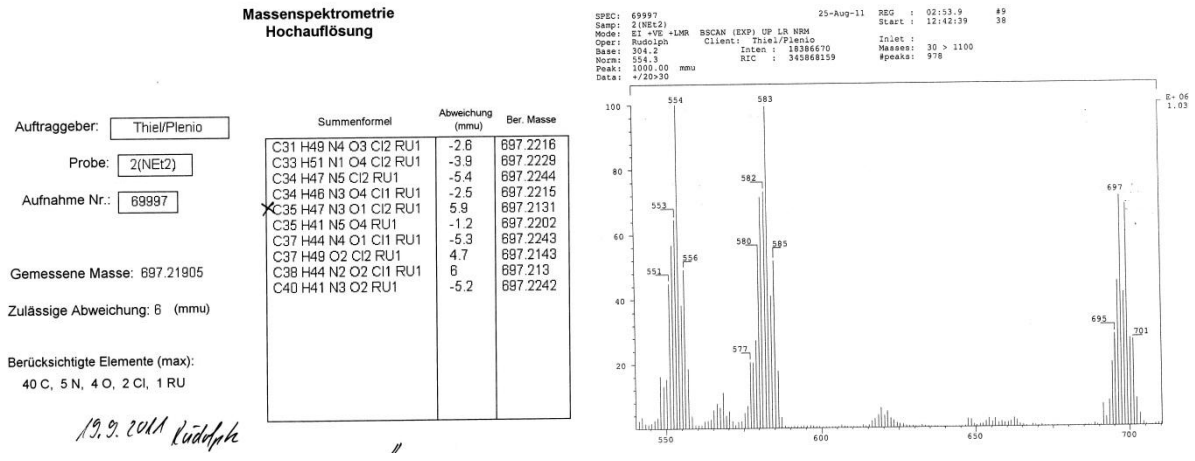

Figure SI-11. Mass spectrometry of **2(NEt$_2$)**.

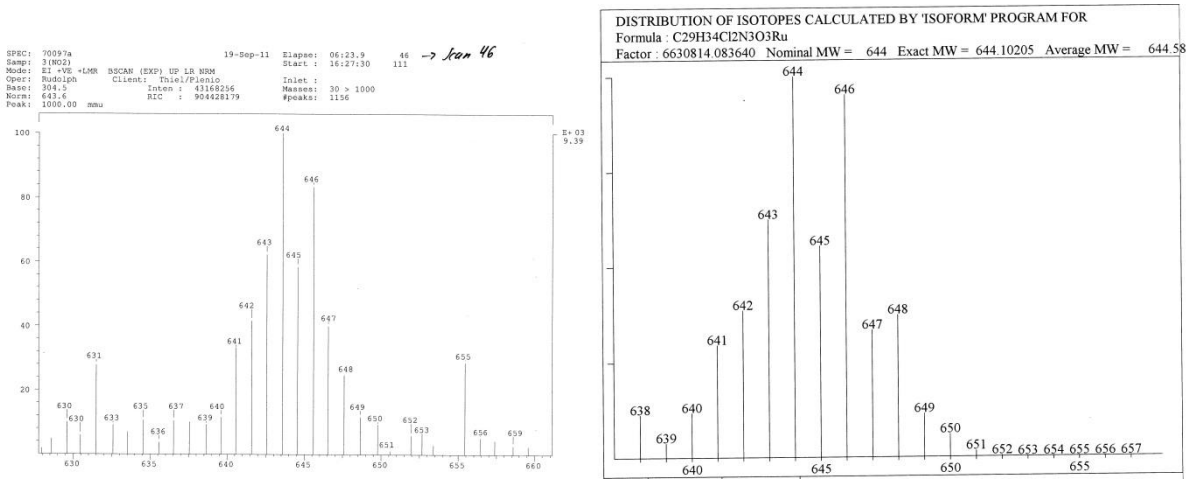

Figure SI-12. Mass spectrometry of **3(NO$_2$)**.

Cyclic voltammograms

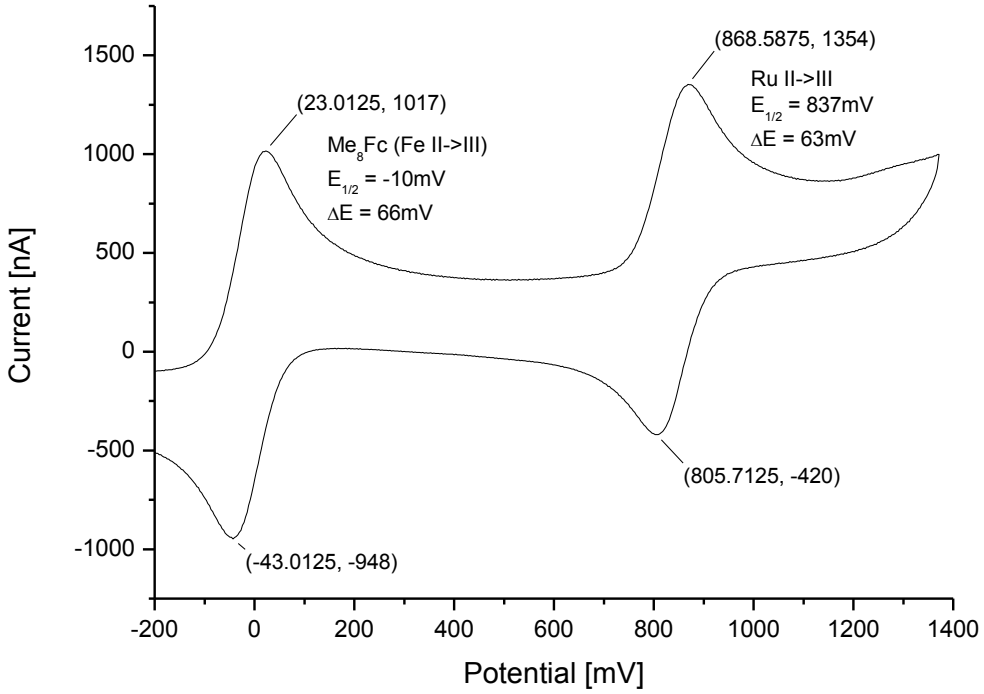

Figure SI-13. Cyclic voltammogram of **1(H)**.

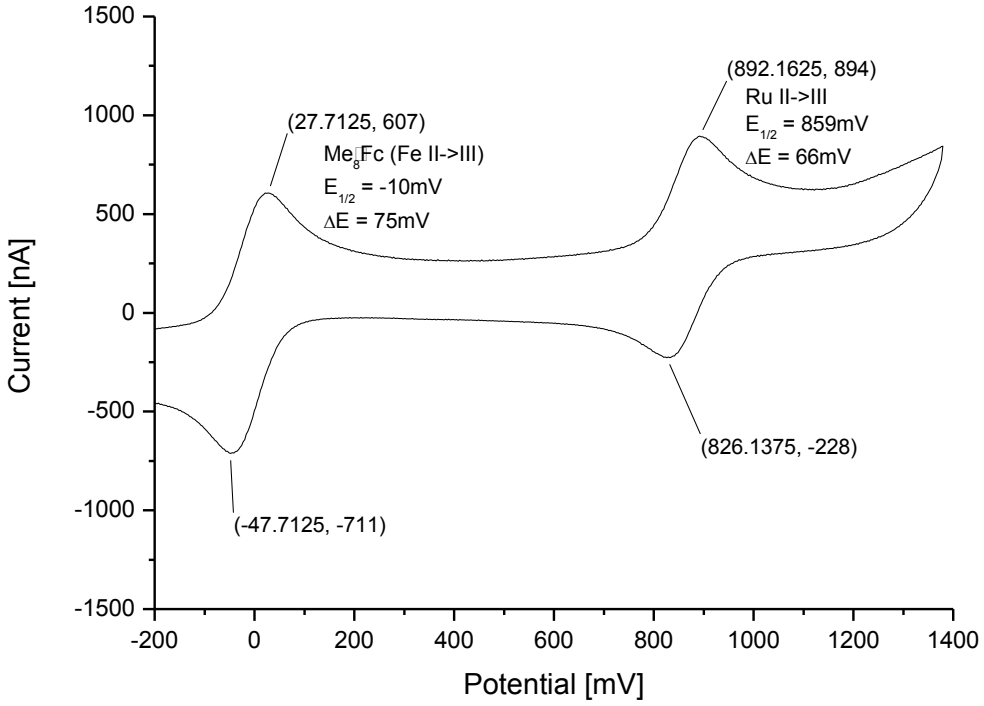

Figure SI-14. Cyclic voltammogram of **1(F)**.

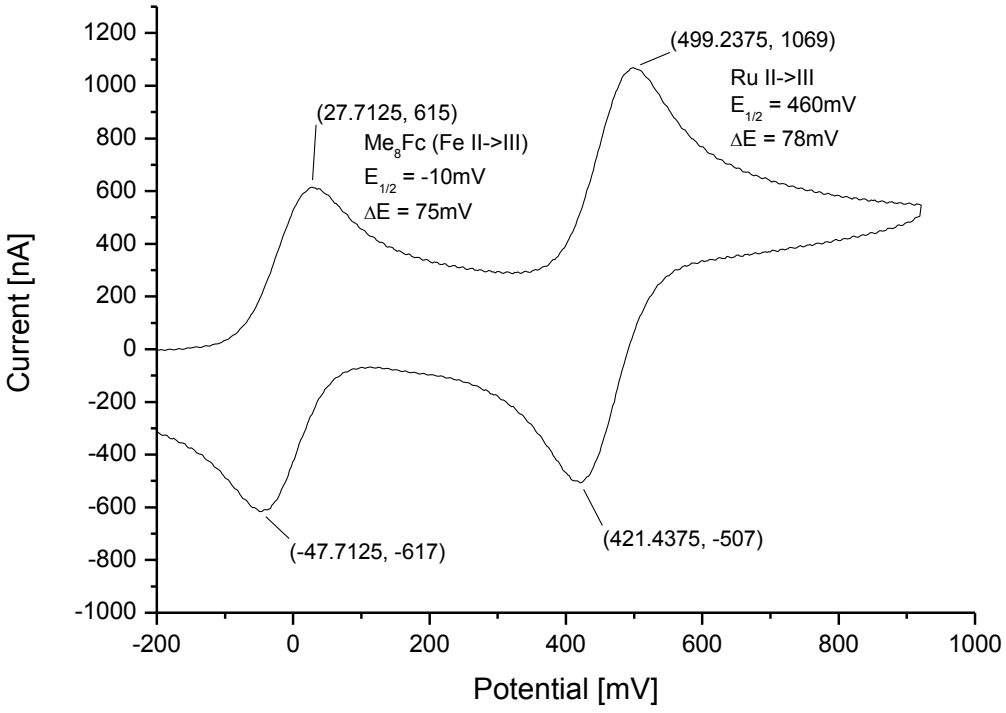

Figure SI-15. Cyclic voltammogram of **1(NEt$_2$)**.

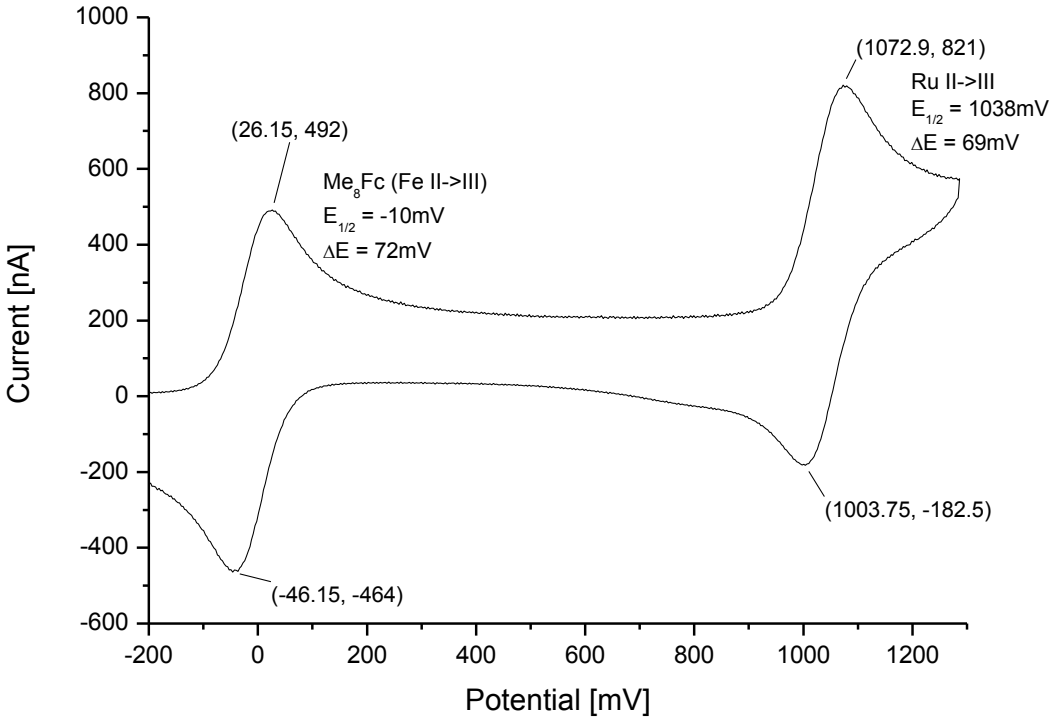

Figure SI-16. Cyclic voltammogram of **1(NO$_2$)**.

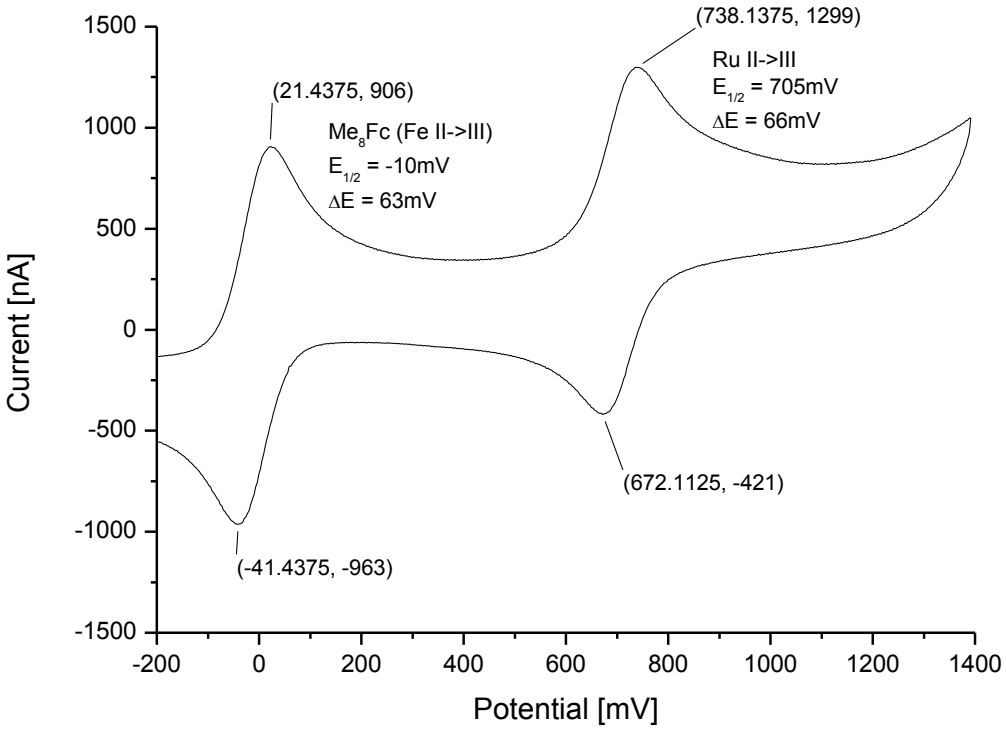

Figure SI-17. Cyclic voltammogram of **1(OiPr)**.

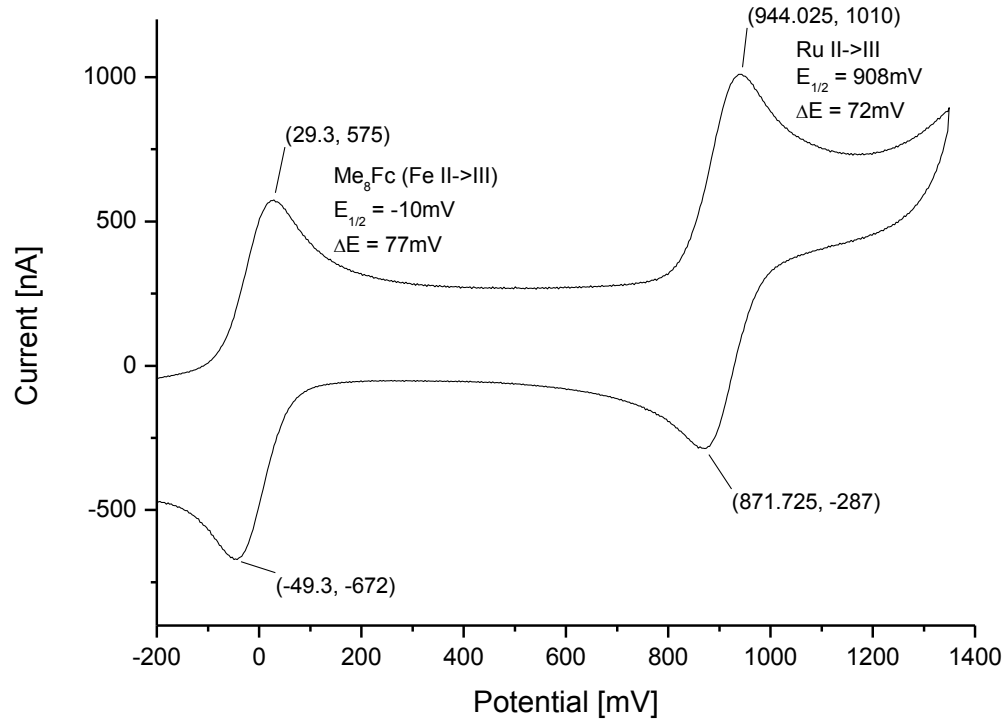

Figure SI-18. Cyclic voltammogram of **2(F)**.

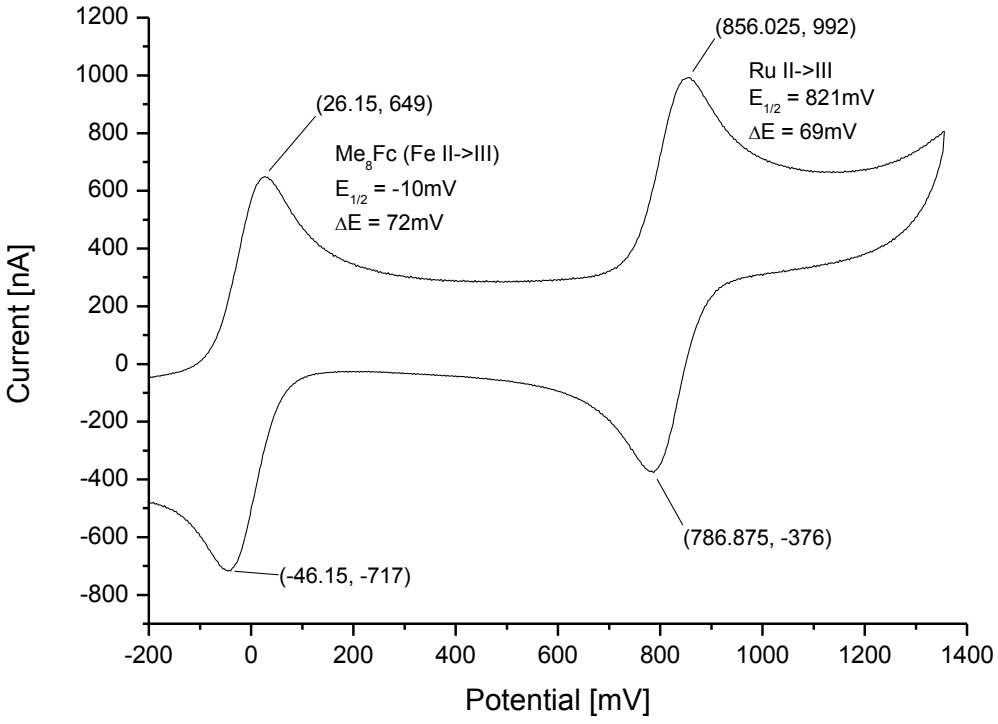

Figure SI-19. Cyclic voltammogram of **2(Me)**.

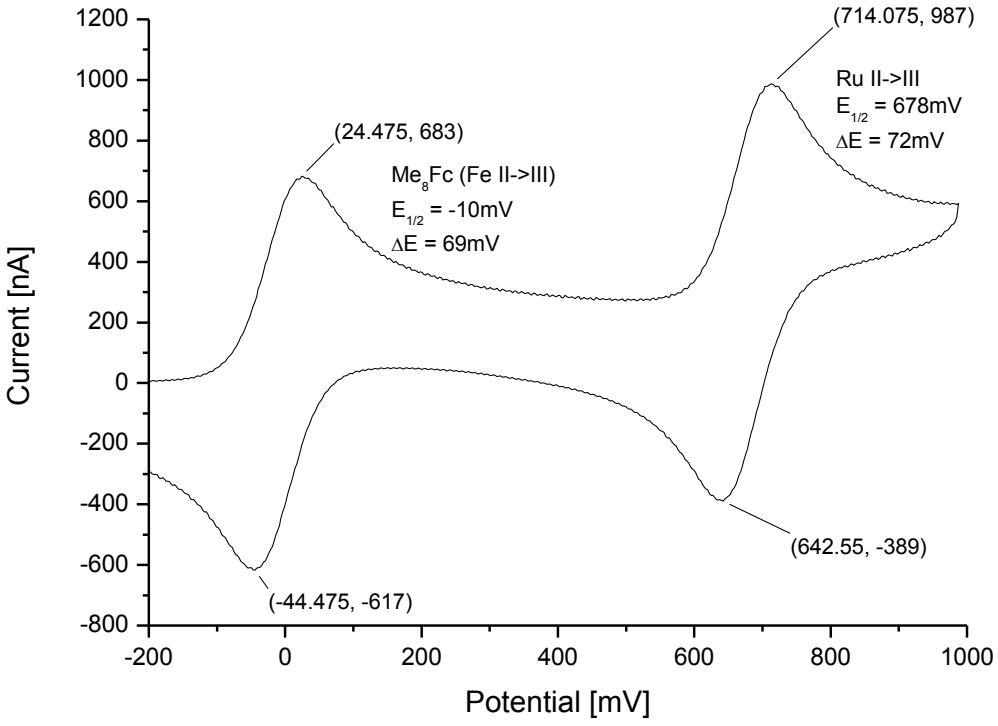

Figure SI-20. Cyclic voltammogram of **2(NEt$_2$)**.

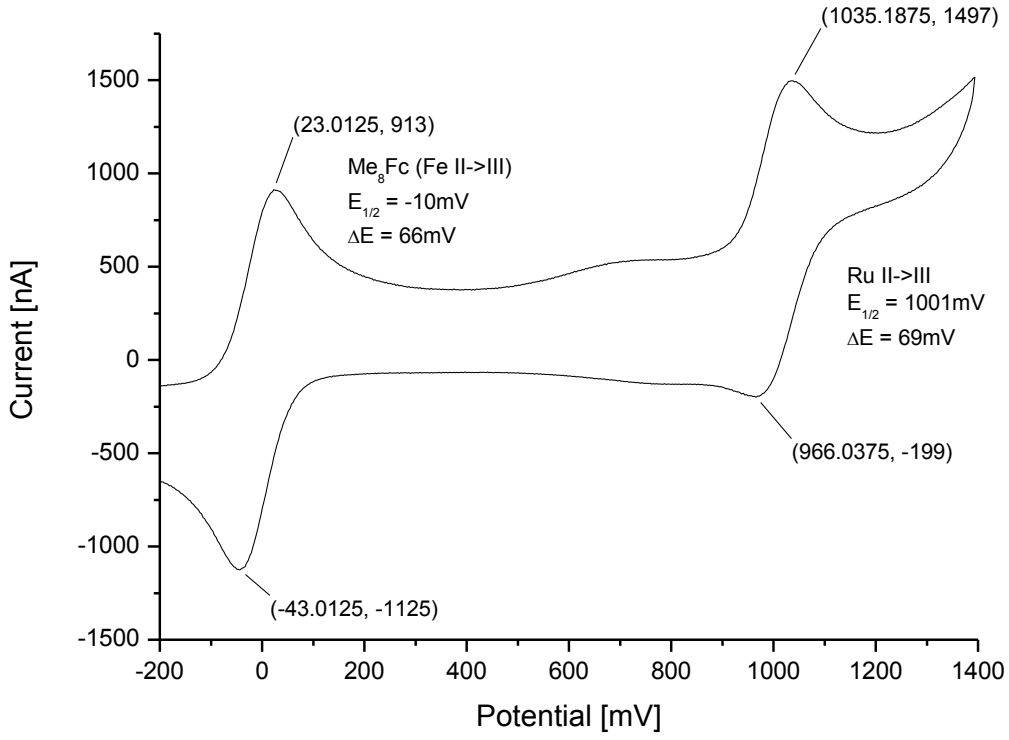

Figure SI-21. Cyclic voltammogram of **2(NO$_2$)**.

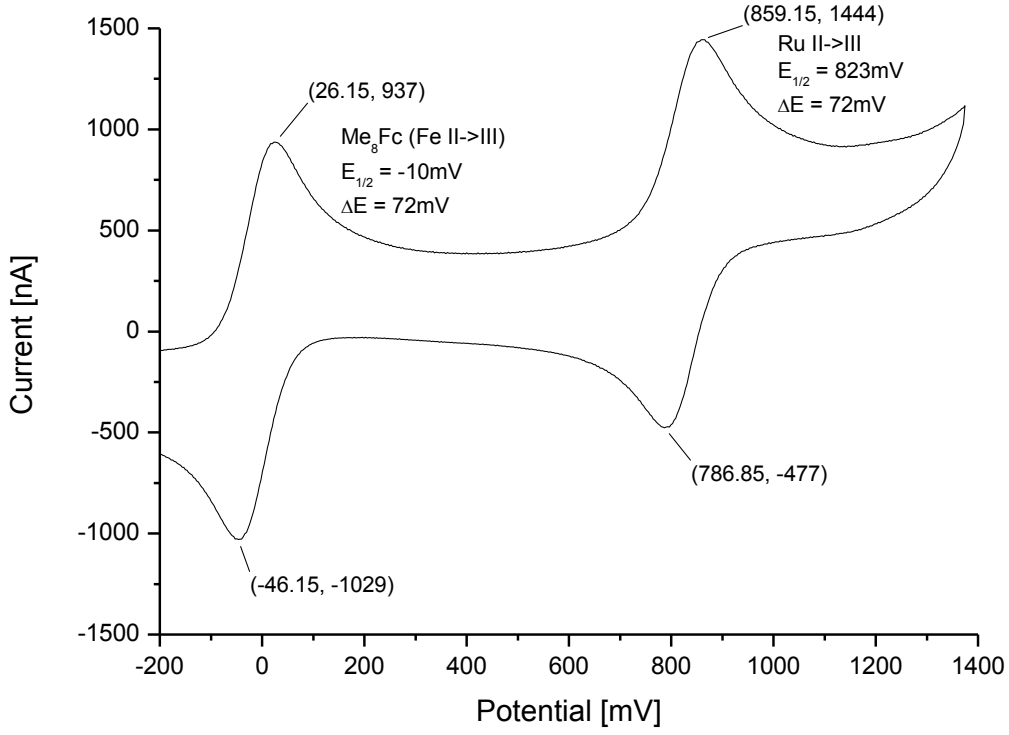

Figure SI-22. Cyclic voltammogram of **2(OiPr)**.

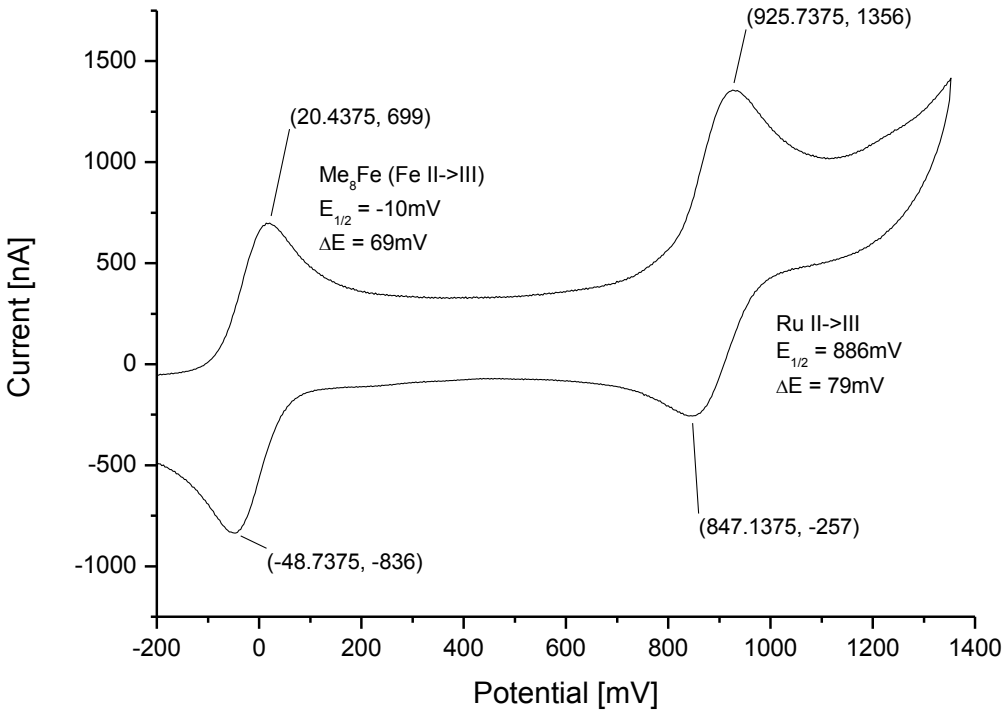

Figure SI-23. Cyclic voltammogram of **3(H)**.

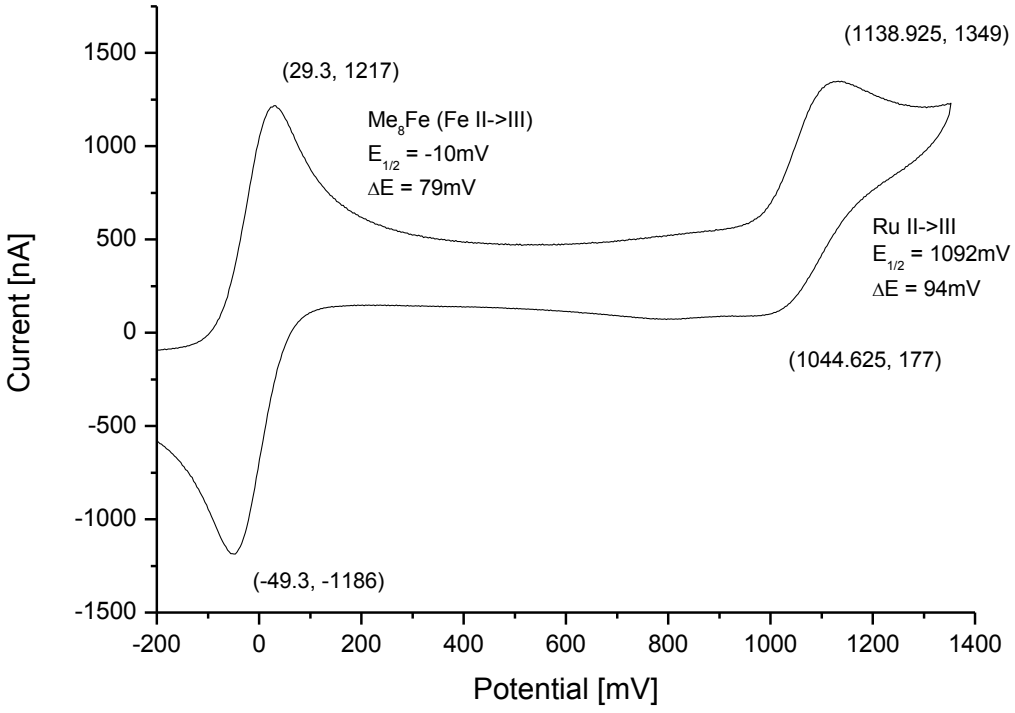

Figure SI-24. Cyclic voltammogram of **3(NO_2)**.

General reaction conditions for the determination of the equilibrium constant of complexes 1, 2, and 3 with PCy_3

A 10 mL Schlenk tube was charged with the respective Grubbs-Hoveyda complex (10^{-6} mol) and PCy_3 ($2.4•10^{-6}$ – $1.6•10^{-5}$ mol; the used amount was calculated from the associated UV/Vis based constants targeting an equal mixture of the precatalyst and the corresponding PCy_3 adduct). The tube was then evacuated and charged with argon (3 cycles). Dry and degassed toluene-d_8 (1 mL) was introduced into the tube. The resulting solution was stirred at 30 °C for at least 6h to establish the equilibrium. The solution was transferred to a NMR tube, kept at 30 °C until the NMR spectra were measured at the same temperature.

The equilibrium constant was calculated from the ratio of the NMR integrals of precatalyst and respective "Grubbs 2nd generation like" complex and the applied [PCy_3].

	integral precatalyst	**integral PCy_3 adduct**	**ratio**	**c(PCy_3) [mol • L^{-1}]**	**K_D [L • mol^{-1}]**
1(H)	0.6820	0.9987	1.464	0.016	92
1(F)	0.6208	1.0725	1.728	0.0024	720
1(NO2)	0.3855	1.0000	2.594	0.0028	926
1(NEt2)	0.6901	1.0000	1.449	0.0122	119
1(OiPr)	0.3900	1.0000	2.564	0.009	285
2(Me)	2.7100	1.0000	0.369	0.0035	105
2(F)	1.0300	1.0000	0.971	0.005	194
2(NO2)	0.5100	1.0000	1.961	0.0038	516
2(NEt2)	0.7900	1.0000	1.266	0.0131	97
2(OiPr)	0.4300	1.0000	2.325	0.0129	180
3(H)	5.1900	1.0000	0.193	0.0022	88
3(NO2)	1.0000	0.7700	1.299	0.0014	928

Table SI-1. Data for the determination of the equilibrium constant of complexes **1**, **2**, and **3** with PCy3.

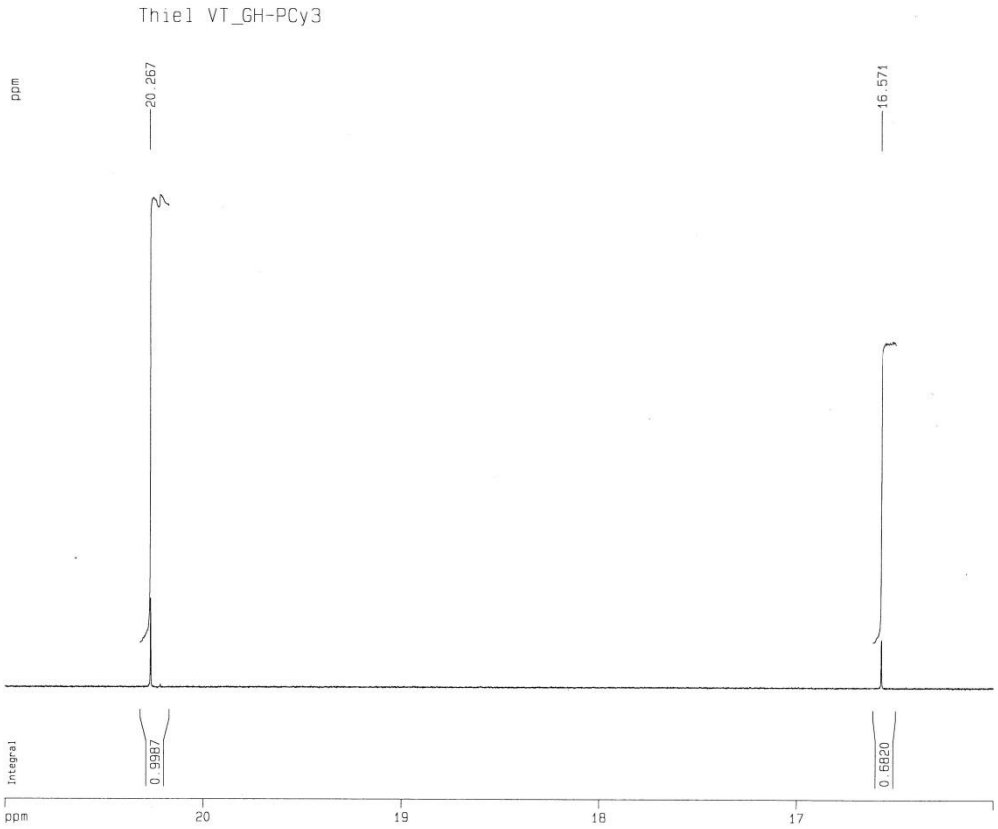

Figure SI-25. ^{1}H NMR spectrum of **1(H)** with PCy_3.

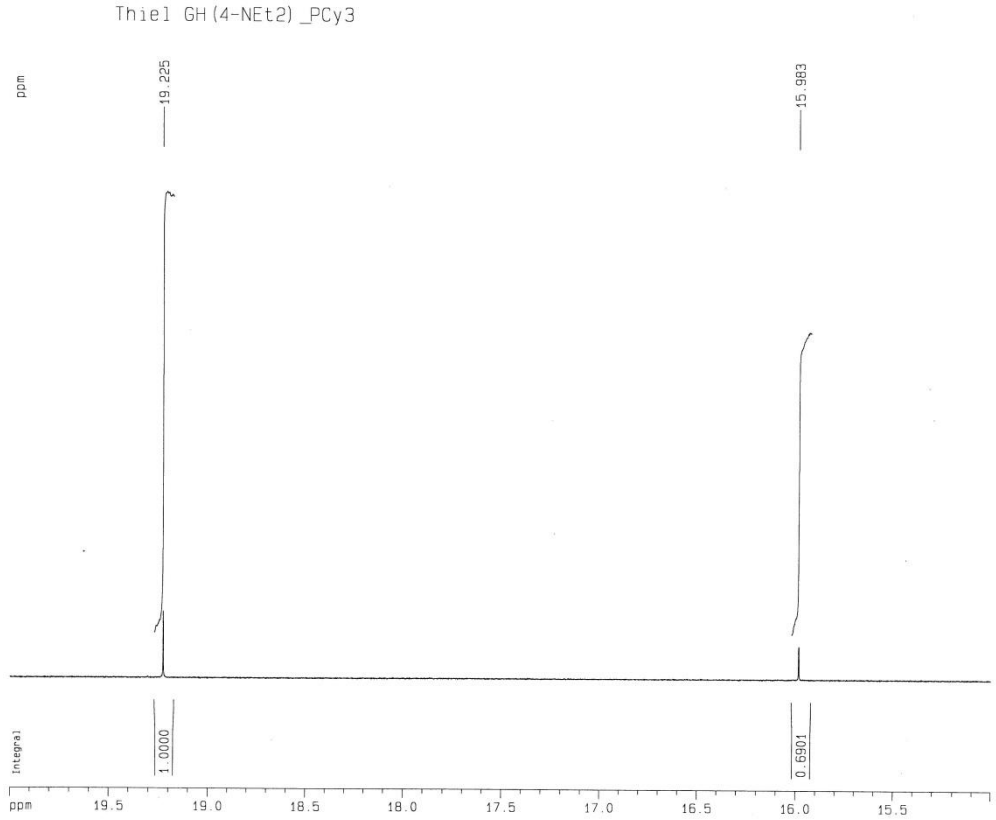

Figure SI-26. ^{1}H NMR spectrum of **1(NEt_2)** with PCy_3.

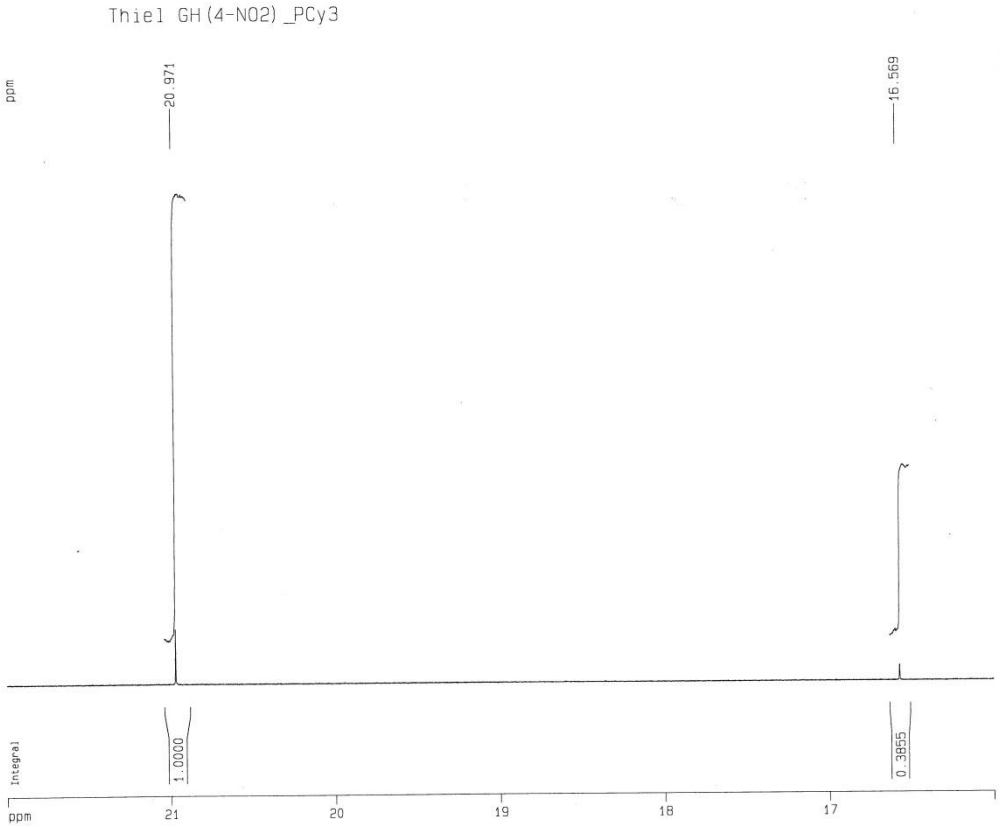

Figure SI-27. ^{1}H NMR spectrum of **1(NO$_2$)** with PCy$_3$.

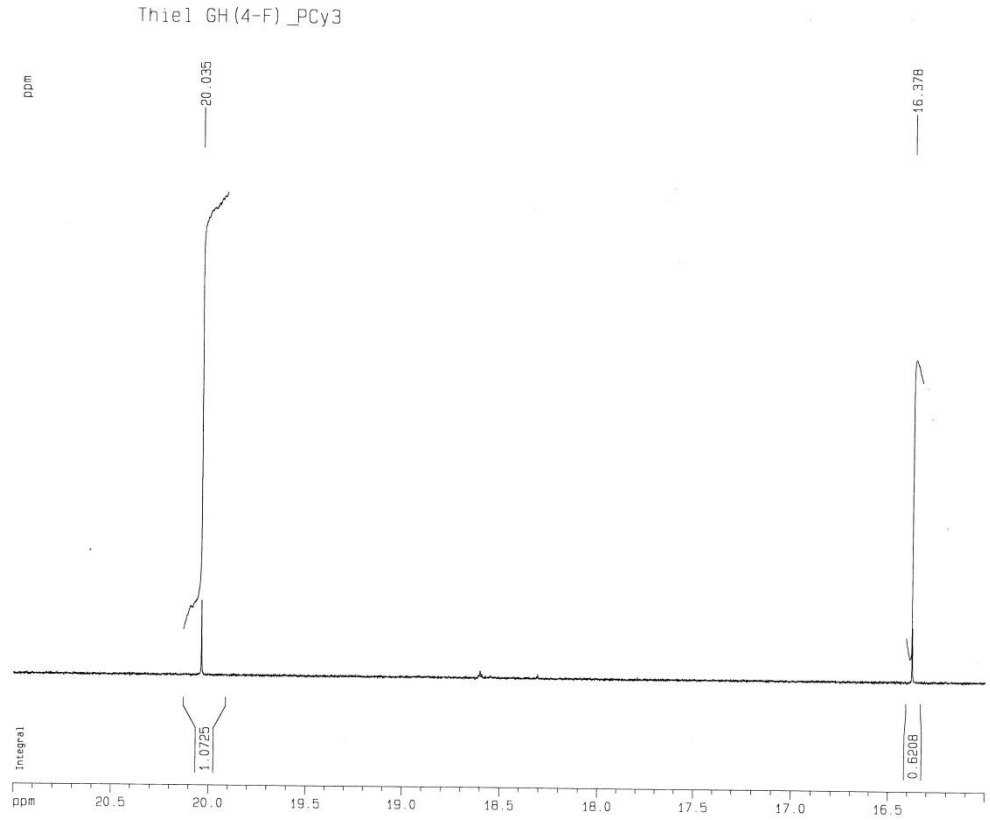

Figure SI-28. ^{1}H NMR spectrum of **1(F)** with PCy$_3$.

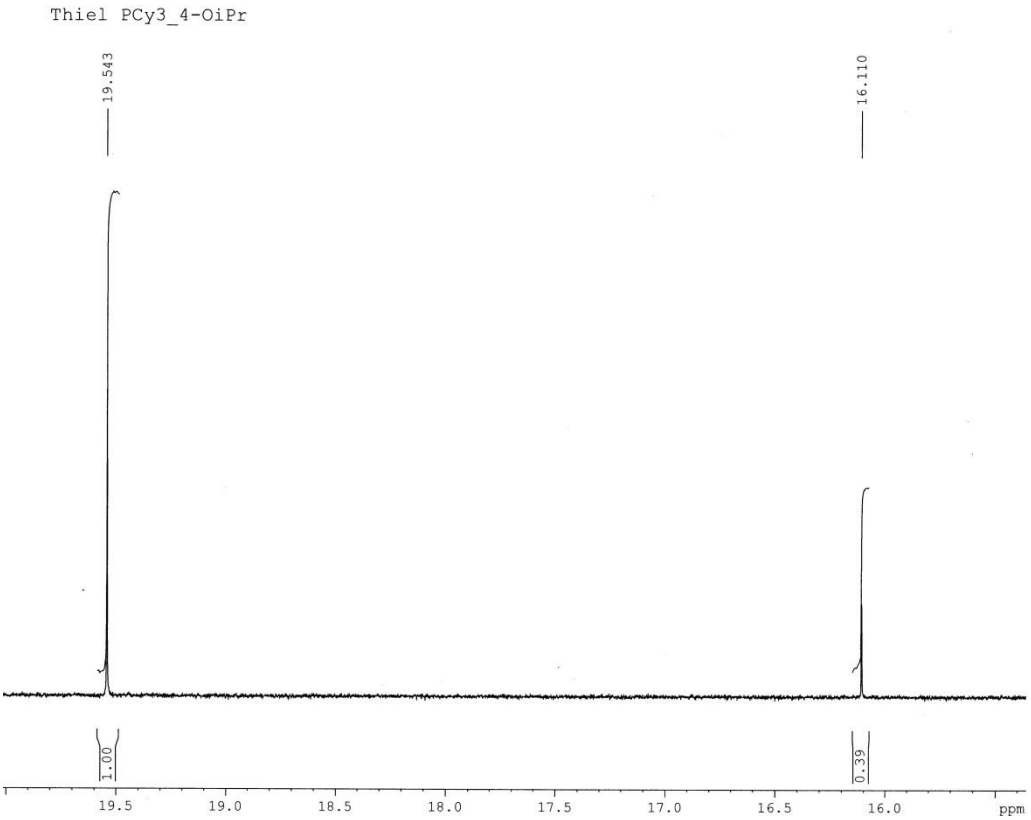

Figure SI-29. ^{1}H NMR spectrum of **1(OiPr)** with PCy_3.

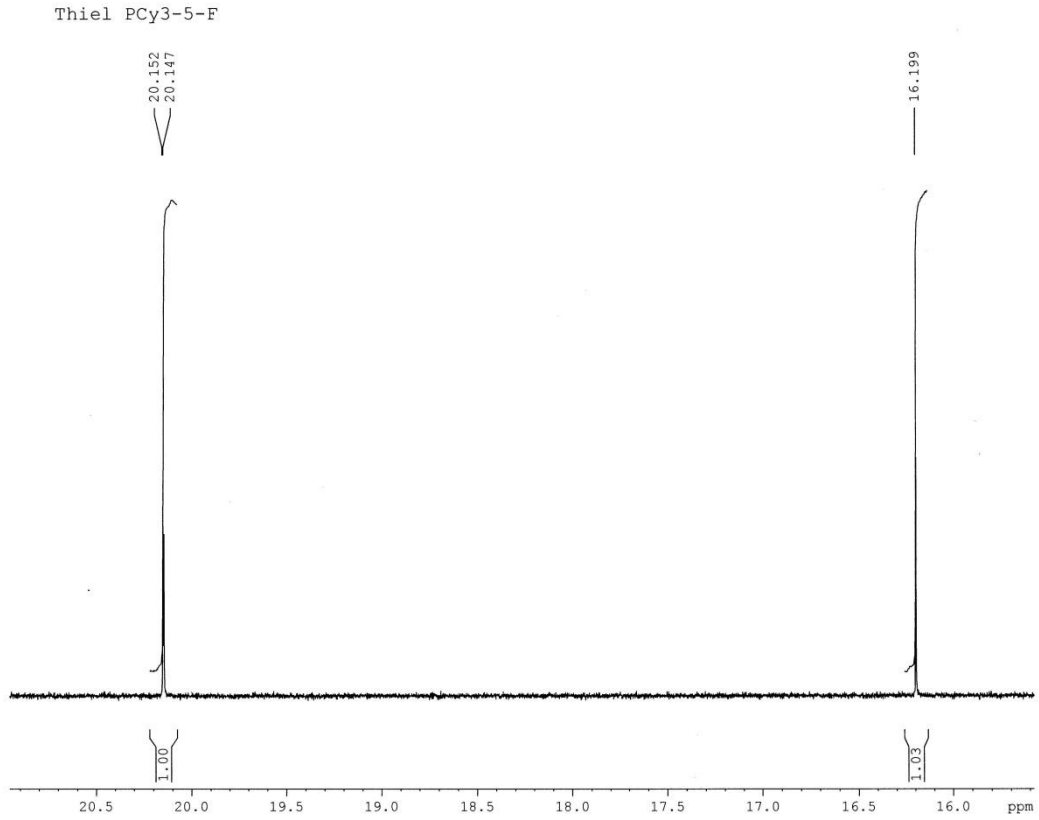

Figure SI-30. ^{1}H NMR spectrum of **2(F)** with PCy_3.

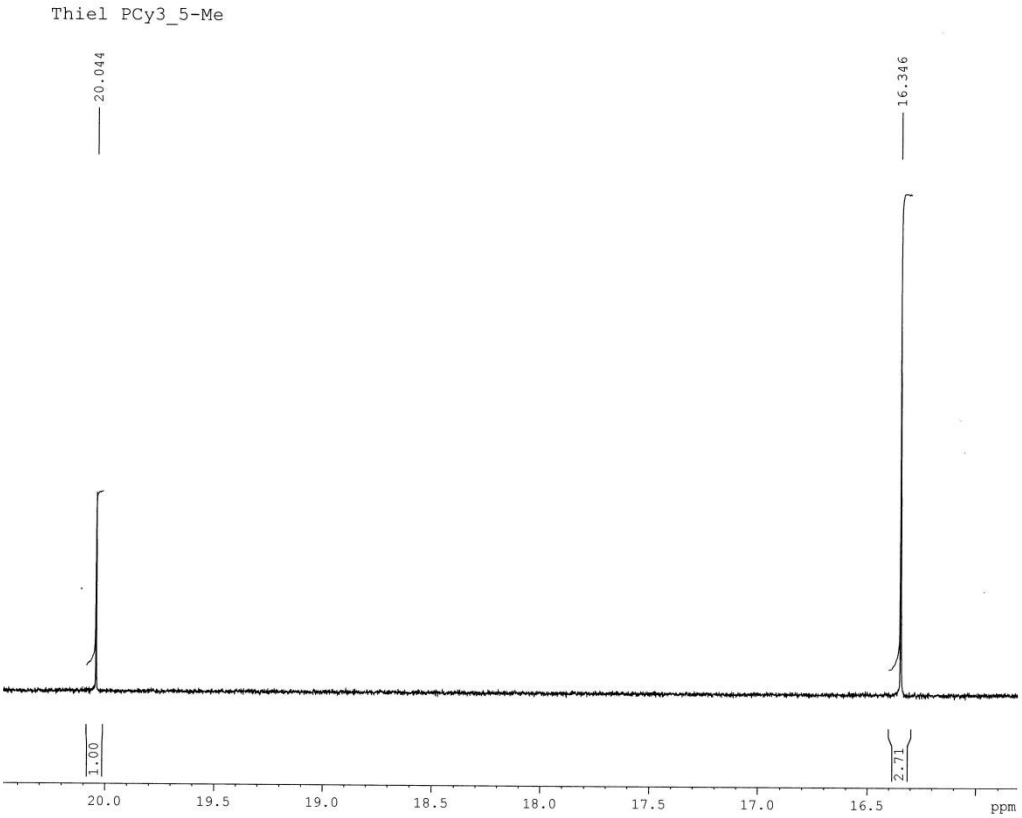

Figure SI-31. ^{1}H NMR spectrum of **2(Me)** with PCy_3.

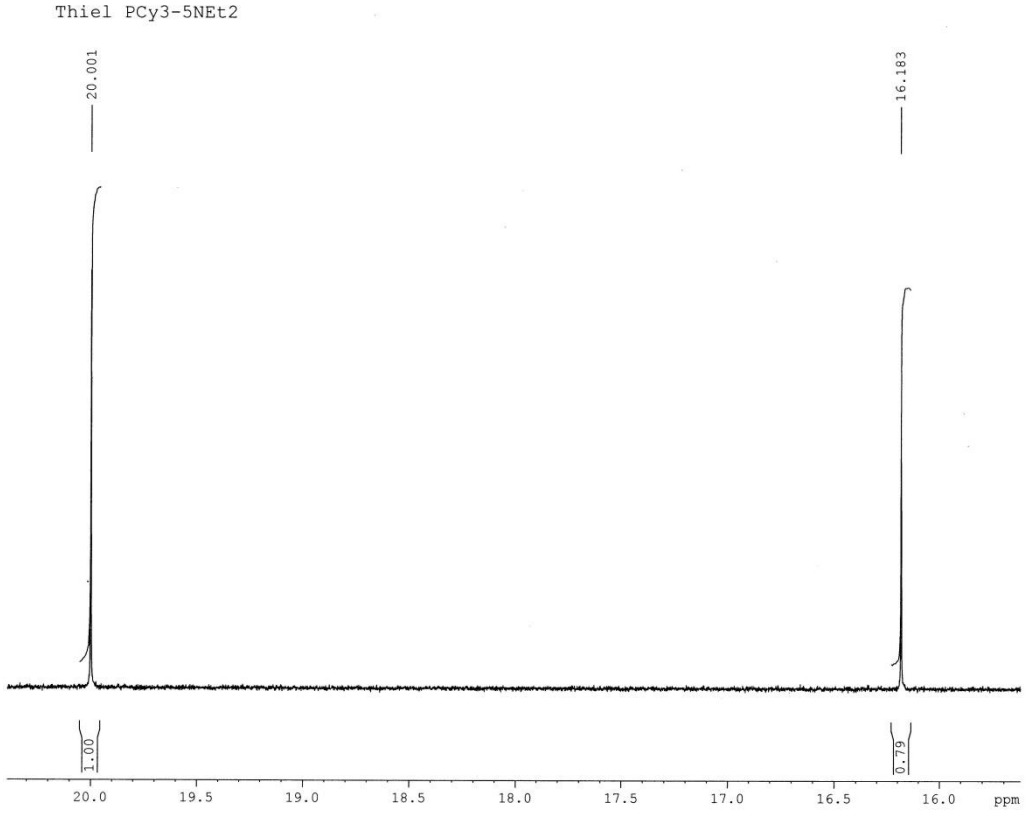

Figure SI-32. ^{1}H NMR spectrum of **2(NEt_2)** with PCy_3.

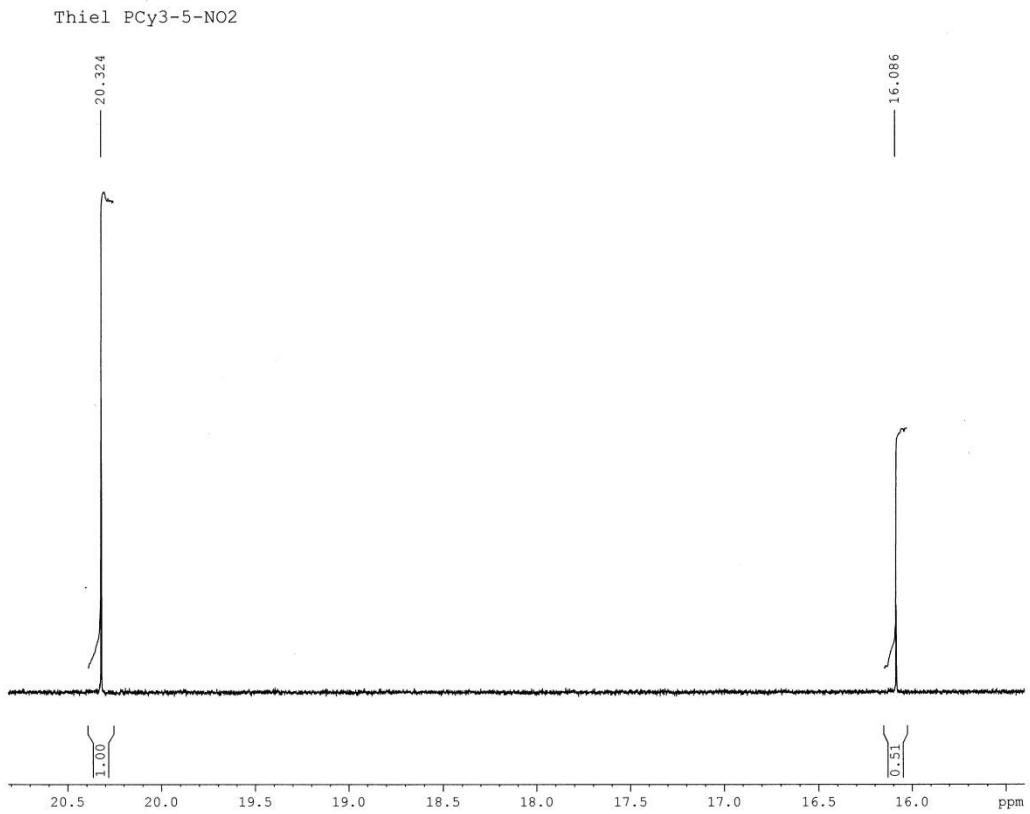

Figure SI-33. ^{1}H NMR spectrum of **2(NO$_2$)** with PCy$_3$.

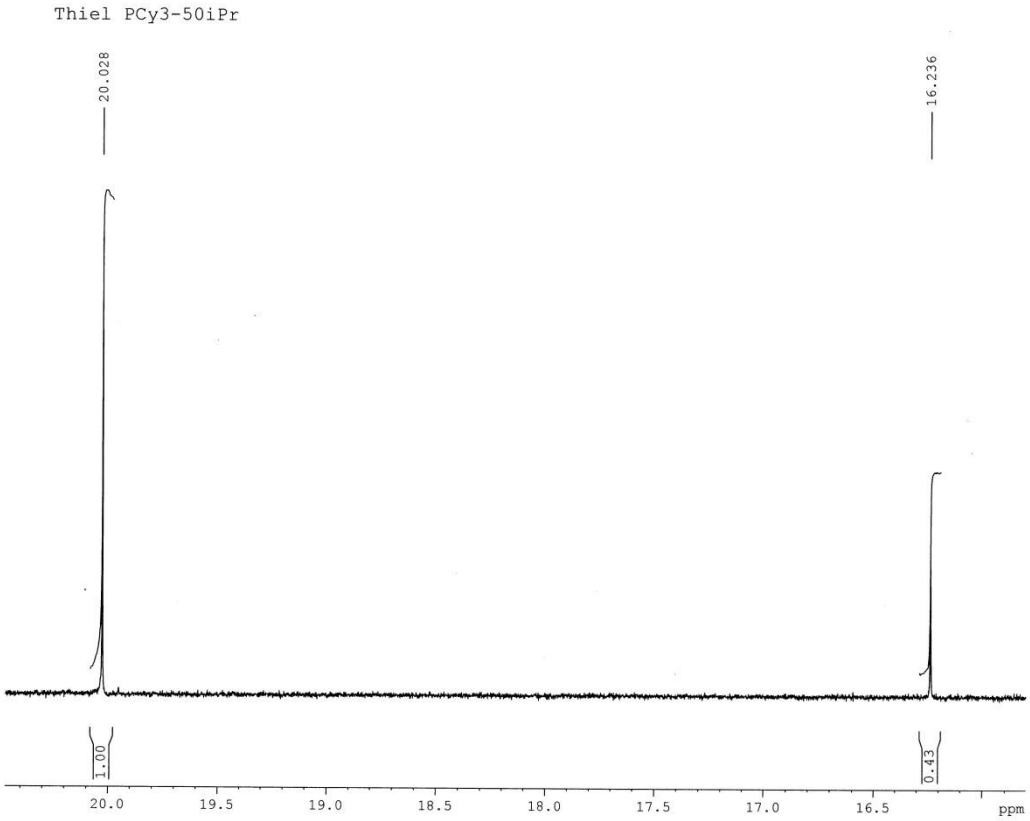

Figure SI-34. ^{1}H NMR spectrum of **2(OiPr)** with PCy$_3$.

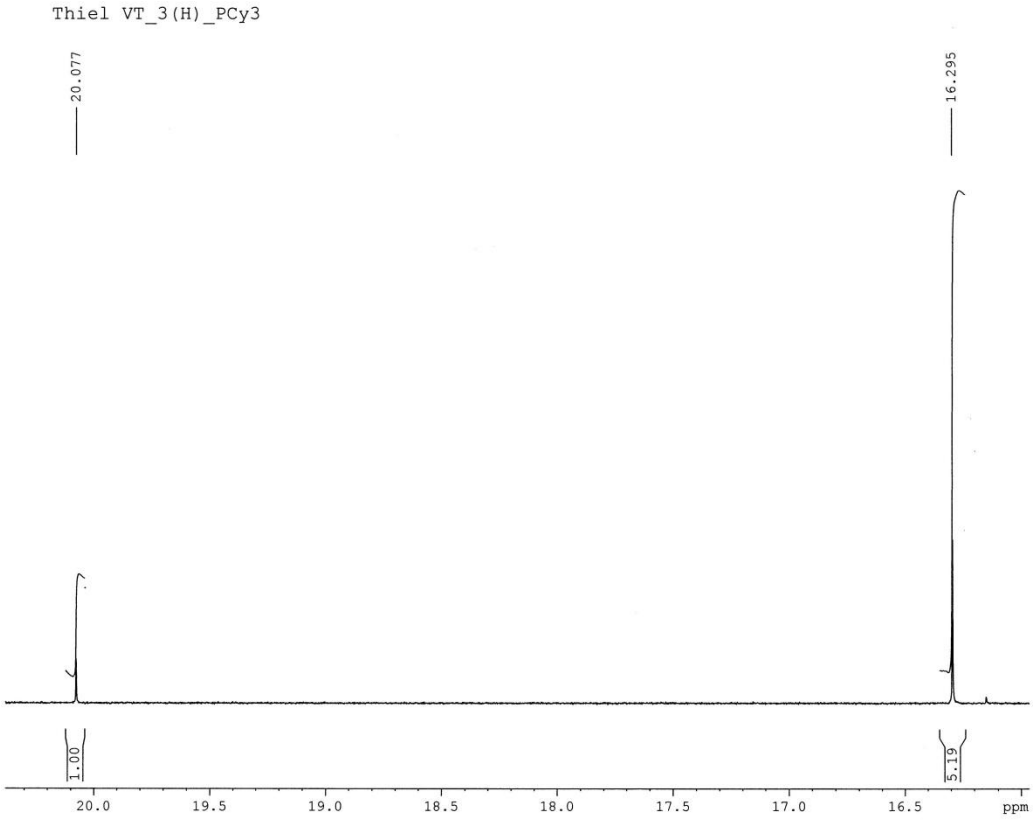

Figure SI-35. ^{1}H NMR spectrum of **3(H)** with PCy_3.

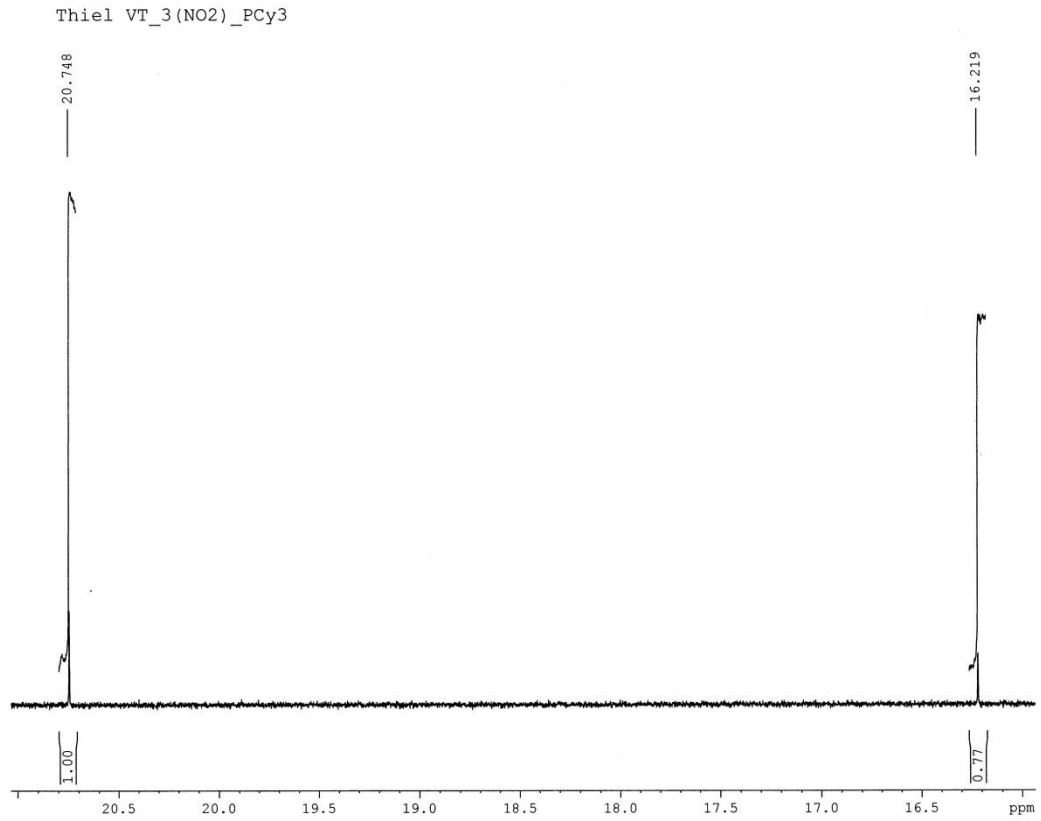

Figure SI-36. ^{1}H NMR spectrum of **3(NO_2)** with PCy_3.

Formal Kinetics

Some experiments were done under conditions where a significant amount of substrate is converted into the product during the initiation period (**method 2nd order**). Then the concentration of substrate changes within the time of experiment and needs to be treated as time dependent in the kinetic model. Other experiments were carried out at very high substrate concentration and consequently relatively low catalyst loading. Under these conditions (**method pseudo 1st order**) only a minor portion of the substrate (within the time of experiment) is converted into the product, consequently, its concentration is nearly constant during the reaction.

Method 2nd order:

Based on the reaction scheme (below) the complex **A** is activated by the substrate S (olefin) to result in complex **B**. **B** then undergoes ruthenacyclobutane formation to **C**, leading after cycloreversion to complex **D.** Following olefin exchange this complex then enters the catalytic cycle as an active catalyst **X**. **X** then allows n-1 (n= TON) substrate molecules to react in fast consecutive steps to the product P. At the end of this sequence an inactive Ruthenium complex (RuC) is obtained.

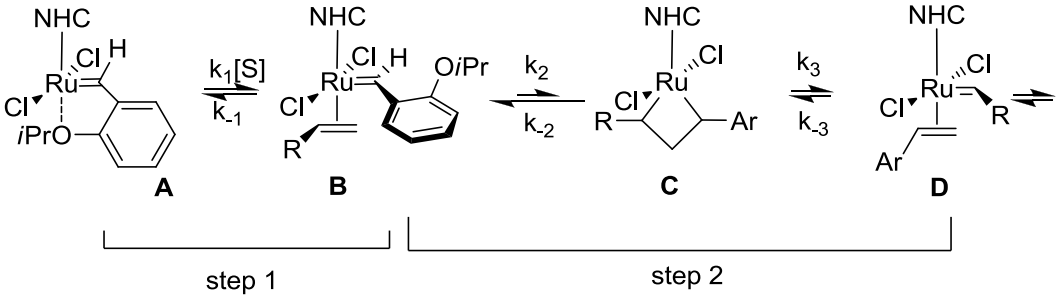

n = TON (turn-over number), X = active catalyst, RuC inactive (decomposed) Ru complex after olefin metathesis

$$A + S \xrightarrow{k} X + P \qquad (1)$$

$$X + (n\text{-}1)\ S \xrightarrow{fast} RuC + (n\text{-}1)\ P \qquad (2)$$

The decrease of the concentration of A is given by (3).

$$-\frac{d[A]}{dt} = k \cdot [A] \cdot [S] \qquad (3)$$

$[A]_{Total}$ is the sum of unactivated A and active catalyst X (see equation (4)).

$$[A]_{Total} = [A] + [X] \qquad (4)$$

$[S]_{Total}$ is the sum of unreacted substrate S and reacted substrate (TON · [X]).

$$[S]_{Total} = [S] + n \cdot [X] \quad (5)$$

It is assumed that one catalyst molecule has a certain TON n (reacts with n molecules of substrate to give n molecules of product P) (6).

$$[S]_{Total} = n \cdot [A]_{Total} \quad (6)$$

Inserting (4) and (5) into (3) results in (7):

$$-\frac{d([A]_{Total} - [X])}{dt} = \frac{d[X]}{dt} = k \cdot ([A]_{Total} - [X]) \cdot ([S]_{Total} - n \cdot [X]) \quad (7)$$

With the use of (6) equation (8) is obtained:

$$\frac{d[X]}{dt} = k \cdot ([A]_{Total} - [X]) \cdot (n \cdot [A]_{Total} - n \cdot [X]) = n \cdot k \cdot ([A]_{Total} - [X])^2 \quad (8)$$

Integration leads to (9) and (10), respectively:

$$\int_0^X \frac{d[X]}{([A]_{Total} - [X])^2} = \int_0^t n \cdot k \cdot dt \quad (9)$$

$$\frac{1}{([A]_{Total} - [X])} - \frac{1}{[A]_{Total}} = n \cdot k \cdot t \quad (10)$$

Replacing X using (4) gives (11):

$$\frac{1}{([A])} - \frac{1}{[A]_{Total}} = n \cdot k \cdot t \quad (11)$$

Rearrangement leads to (12) or (13), respectively:

$$[A] = \frac{[A]_{Total}}{1 + n \cdot k \cdot [A]_{Total} \cdot t} = \frac{[A]_{Total}}{1 + k \cdot [S]_{Total} \cdot t} \quad (12)$$

$$\frac{[A]}{[A]_{Total}} = \frac{1}{1 + k \cdot [S]_{Total} \cdot t} \quad (13)$$

For the UV/VIS measurements Beer´s Law is valid for the absorbance A (14):

$$A = \varepsilon_A \cdot [A] \cdot d + \varepsilon_{RuC} \cdot [RuC] \cdot d \quad (14)$$

The mass balance for the Ruthenium complexes is given by (15). By insertion into (14), (16) is obtained:

$$[A]_{Total} = [A] + [RuC] \quad (15)$$

$$A = \varepsilon_A \cdot [A] \cdot d + \varepsilon_{RuC} \cdot ([A]_{Total} - [A]) \cdot d \quad (16)$$

Rearrangement and substitution of $A_\infty = \varepsilon_{RuC} \cdot [A]_{Total} \cdot d$ leads to (17):

$$A - A_\infty = (\varepsilon_A - \varepsilon_{RuC}) \cdot [A] \cdot d \quad (17)$$

The multiplication by $[A]_{Total}/[A]_{Total}$ yields (18):

$$A - A_\infty = (\varepsilon_A \cdot [A]_{Total} \cdot d - \varepsilon_{RuC} \cdot [A]_{Total} \cdot d) \cdot [A]/[A]_{Total} \quad (18)$$

Using $A_0 = \varepsilon_A \cdot [A]_{Total} \cdot d$ gives (19):

$$\frac{A - A_\infty}{A_0 - A_\infty} = [A]/[A]_{Total} \quad (19)$$

Equilibration with (13) gives ($k_{obs} = k \cdot [S]_{Total}$)

$$\frac{A - A_\infty}{A_0 - A_\infty} = \frac{[A]}{[A]_{Total}} = \frac{1}{1 + k_{obs} \cdot t} \quad (20)$$

The final equation is given by (21).

$$A = \frac{A_0 - A_\infty}{1 + k_{obs} \cdot t} + A_\infty \quad (21)$$

Method pseudo 1st order:

The decrease of the concentration of GH is given by (23).

$$-\frac{d[A]}{dt} = k \cdot [A] \cdot [S] \quad (23)$$

The balance equations are given by (24) – (25):

$[A]_{Total} = [A] + [X]$ (24)

$[S]_{Total} = [S] + n \cdot [X]$ (25)

Because of the high excess of the substrate, $n \cdot [X]$ is negligible as compared to [S] ($n \cdot [X] \ll [S]$). The concentration of the substrate remains approximately constant during an experiment (26).

$[S]_{Total} \approx [S]$ (26)

Inserting (26) into (23) results in (B7):

$$-\frac{d[A]}{dt} = k \cdot [A] \cdot [S]_{Total} = k_{obs} \cdot [A] \quad \text{(B7)}$$

Integration leads to (28):

$$[A] = [A]_{Total} \cdot e^{-k_{obs} \cdot t} = [A]_{Total} \cdot e^{-k \cdot [S]_{Total} \cdot t} \quad (28)$$

Similar considerations lead to the final equations (29) and B(30) used for the fit of the UV/Vis measurements.

$$A = (A_0 - A_\infty) \cdot e^{-k_{obs} t} + A_\infty \quad (29)$$

$$I = (I_0 - I_\infty) \cdot e^{-k_{obs} t} + I_\infty \quad (30)$$

General conditions for the UV/Vis experiments

All experiments were done in quarz cuvettes 110-QS with a path length of 10.00 mm. The temperature (30 °C unless otherwise noted) was adjusted using a thermostat and controlled with a digital thermometer. Diethyl diallyl malonate (DEDAM), styrene, n-butyl vinyl ether (BuVE), 1-hexene, neohexene, and PCy_3 were used as substrates for measurements.

The following general procedure was applied in all experiments: $1.00 \cdot 10^{-5}$ mol of precatalyst was dissolved in abs. toluene (50 mL) to give a $2.00 \cdot 10^{-4}$ M solution. 1500 µL of this stock solution were filled in a cuvette and an additional amount of toluene was added. This amount was calculated in a way that, after the addition of substrate, the precatalyst concentration is $1.00 \cdot 10^{-4}$ M. The cuvette was then placed in the spectrometer and was allowed to adjust to the respective temperature. The measurement was started in the moment of the addition of the corresponding amount of preheated (same temperature as inside the cuvette) substrate. During the measurement the cuvette was closed with a PTFE stopper (not gas tight).

Reactions with n-butyl vinyl ether (BuVE)

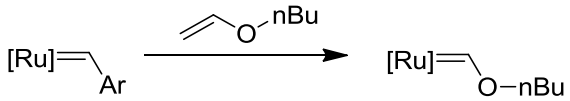

Reactions with n-butyl vinyl ether only perform a single catalytic cycle resulting in a metathesis inactive Fischer carbene. Consequently, the substrate concentration remains virtually constant even at low initial substrate concentration. Therefore only **method pseudo 1st order** was used in the kinetic treatment. To determine k_{obs} at different BuVE concentrations (0.01 to 3.5 M) the initiation reaction of the precatalyst was monitored by recording time-dependent UV/Vis spectra. For the interpretation of the kinetic data obtained at the precatalyst's LMCT band, the absorbance – time traces were fitted with an exponential function (for the k_{obs} values see table-SI2). As representative examples the UV/Vis traces and absorbance – time curves for **1(H)** and 0.5 M BuVE are shown in figure SI-37. The other complexes and substrate concentrations behave accordingly.

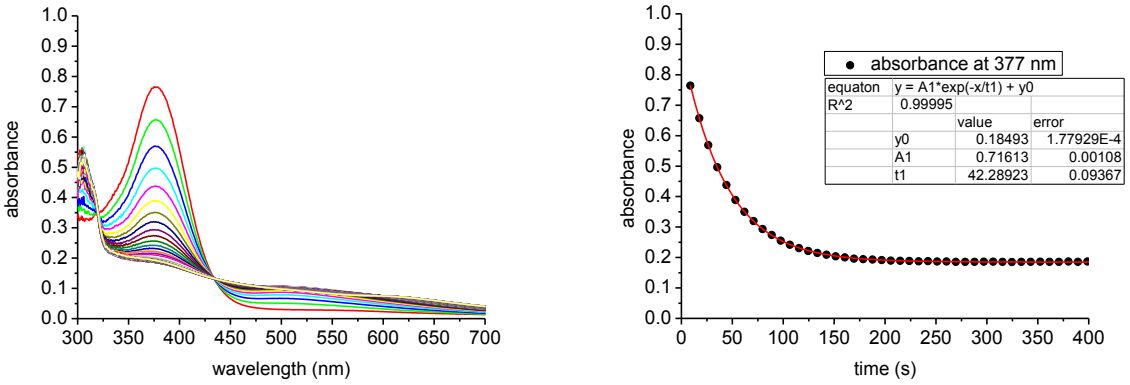

Figure SI-37. Left: UV/Vis traces of **1(H)** ($1.00 \cdot 10^{-4}$ M) with reaction with BuVE (0.5 M). Spectra are recorded with Δt = 9 s. Right: Corresponding absorbance – time curves at 377 nm. The data are fitted using ($y = A1 \cdot \exp(-x/t1) + y0$) and ($k_{obs} = 1/t1$).

The k_{obs} vs. [BuVE] plots are shown in figure SI-38.

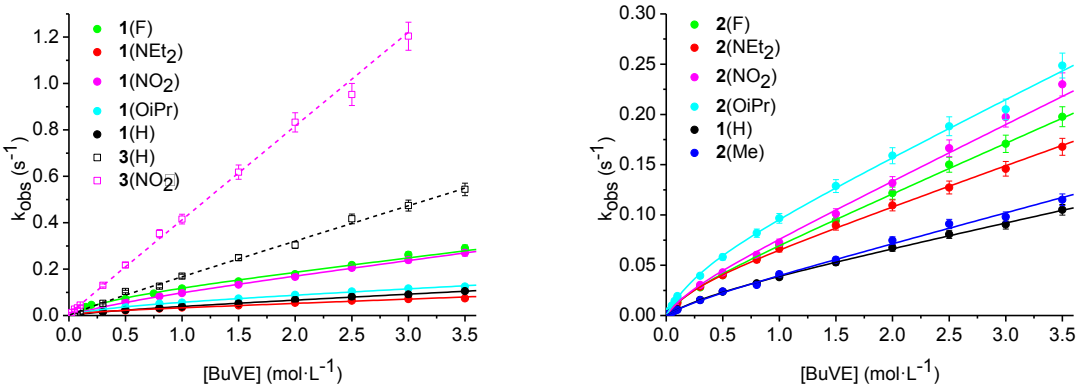

Figure SI-38 Left: k_{obs} vs. [BuVE] plots for complexes **1** and **3**. Right: k_{obs} vs. [BuVE] plots for complexes **2**. The data are fitted using (y = a·b·x/(1+b·x)+c·x) for complexes **1** and **2** and (y = c·x) for complexes **3**.

c(BuVE) [M]	**1(H)**	**1(F)**	**1(NO_2)**	**1(OiPr)**	**1(NEt_2)**	**2(F)**	**2(NO_2)**	**2(OiPr)**	**2(NEt_2)**	**2(Me)**	**3(H)**	**3(NO_2)**
0.01	0.00064	0.00283	0.00168	0.0013	0.00124	0.00149	0.00145	0.00207	0.00161	0.00072	0.00221	0.00529
0.025	0.00164	0.00554	0.00338	0.00301	0.00275	0.00352	0.0034	0.0046	0.00343	0.00153	0.00494	0.01303
0.05	0.00325	0.01147	0.00695	0.0063	0.00495	0.00697	0.00696	0.00977	0.00676	0.00282	0.01077	0.02737
0.075	0.00478	0.01792	0.01017	0.00864	0.00699	0.01048	0.01076	0.01447	0.00952	0.00459	0.01457	0.03284
0.1	0.00618	0.02416	0.01323	0.01169	0.00866	0.0139	0.0172	0.01925	0.01227	0.00565	0.0197	0.0445
0.3	0.01543	0.04558[a]	0.03745	0.02558	0.01649	0.02787	0.03038	0.03945	0.02861	0.01531	0.05253	0.12991
0.5	0.02365	0.07174	0.05768	0.03684	0.02104	0.04007	0.04287	0.05816	0.04002	0.02391	0.10355	0.21737
0.8	0.03201	0.09451[b]	0.08279	0.05076	0.02987	0.05701	0.06021	0.08193	0.05548	0.03037	0.12603	0.35277
1.0	0.03812	0.11633	0.09636	0.05565	0.03392	0.0703	0.07237	0.09665	0.06659	0.04107	0.16982	0.41552
1.5	0.05284	0.14685	0.13336	0.07306	0.0437	0.09431	0.10114	0.1288	0.08949	0.05542	0.24937	0.6178
2.0	0.06733	0.17775	0.16661	0.08908	0.05513	0.1217	0.13159	0.15895	0.10955	0.07461	0.30387	0.83261
2.5	0.08075	0.21753	0.20513	0.1032	0.06387	0.15001	0.16638	0.18821	0.12735	0.09114	0.41654	0.9527
3.0	0.0906	0.26156	0.23911	0.11649	0.07049	0.17082	0.19731	0.20502	0.14592	0.09807	0.47398	1.20381
3.5	0.10522	0.29005	0.27016	0.12441	0.07404	0.19771	0.22991	0.24864	0.16779	0.11512	0.54363	-

Table SI-2. k_{obs} values for BuVE. Error for measurements is 5%. a) BuVE concentration was 0.2 M. b) BuVE concentration was 0.75 M.

Reactions with diethyl diallyl malonate (DEDAM)

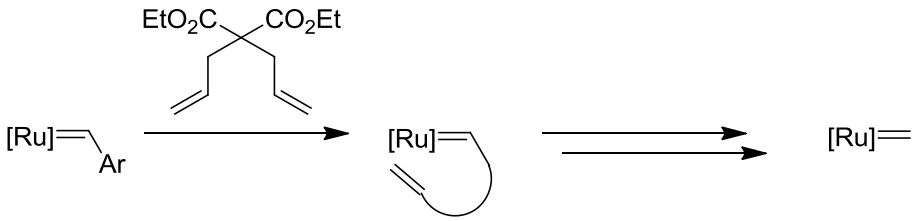

Reactions of diethyl diallyl malonate (DEDAM) with Grubbs-Hoveyda type complexes lead to precatalyst activation, followed by a catalytic reaction, in which an additional number of n DEDAM molecules are converted into the RCM product. Hence the substrate consumption at low concentrations (0.01 – 0.1 M) is relevant during the initiation period **method 2nd order** was used in the kinetic treatment. At higher concentrations (0.25 – 2.0 M) this was no longer relevant and **method pseudo 1st order** was applied. To determine k_{obs} at different DEDAM concentrations (0.01 to 2.0 M) the initiation process of the precatalyst was monitored by recording UV/Vis spectra to follow the spectral changes with time. The precatalyst's LMCT band absorbance – time traces were fitted either with an exponential function or with a hyperbolic function (for the k_{obs} values see table-SI3). As representative examples the UV/Vis traces and absorbance – time curves for **1(F)** with 0.025 M and 1.0 M DEDAM are shown in figures SI-39 and SI-40. The other complexes and substrate concentrations behave accordingly.

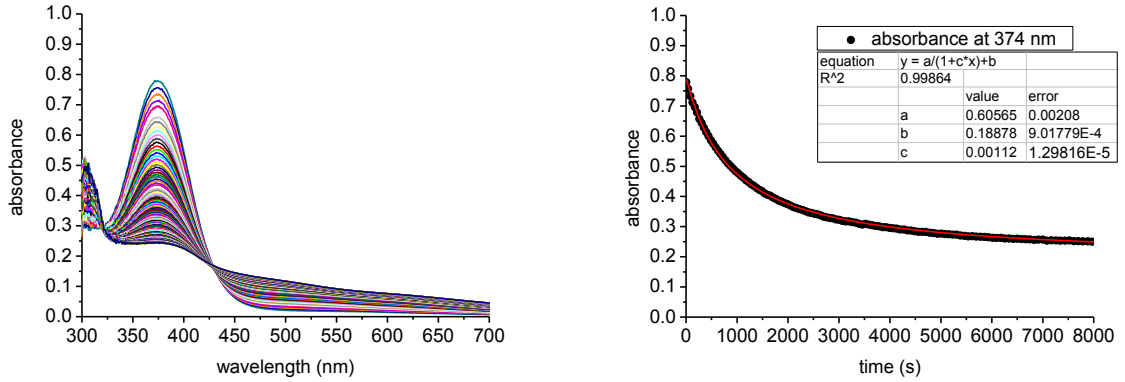

Figure SI-39. Left: UV/Vis traces of **1(F)** ($1.00 \cdot 10^{-4}$ M) with reaction with DEDAM (0.025 M). Spectra are recorded with Δt = 40 s. Right: Corresponding absorbance – time curves at 374 nm. The data are fitted using ($y = a/(1+c \cdot x) + b$) and ($k_{obs} = c$).

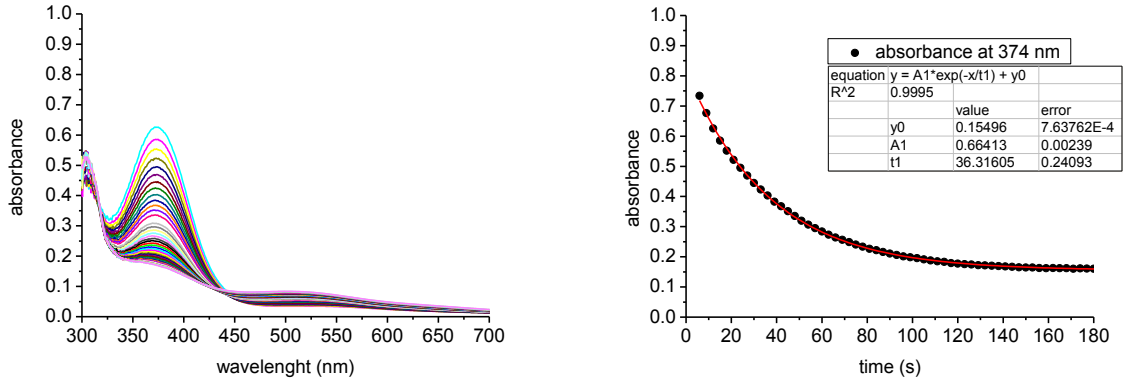

Figure SI-40. Left: UV/Vis traces of **1(F)** (1.00 • 10^{-4} M) with reaction with DEDAM (1.0 M). Spectra are recorded with Δt = 3 s. Right: Corresponding absorbance – time curves at 374 nm. The data are fitted using (y = A1·exp(-x/t1) + y0) and (k_{obs} = 1/t1).

The k_{obs} vs. [DEDAM] plots are shown in figure SI-41.

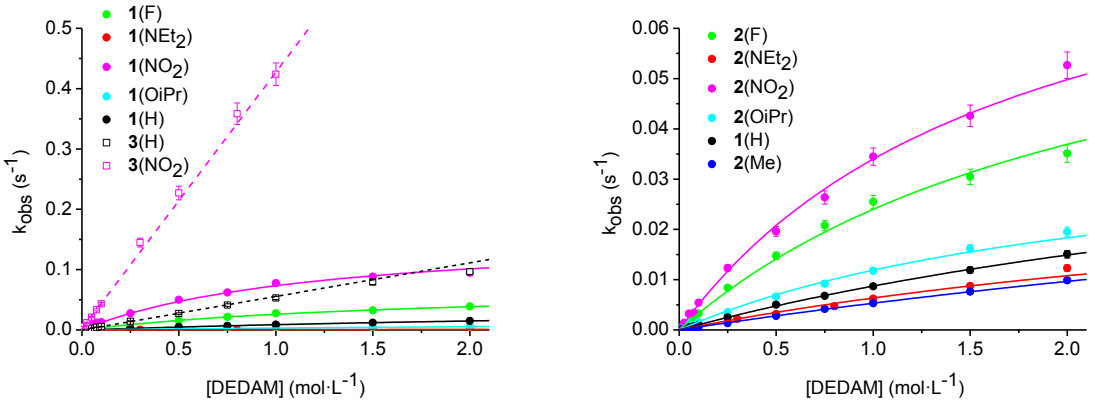

Figure SI-41 Left: k_{obs} vs. [DEDAM] plots for complexes **1** and **3**. Right: k_{obs} vs. [DEDAM] plots for complexes **2**. The data are fitted using (y = a·b·x/(1+b·x)) for complexes **1** and **2** and (y = c·x) for complexes **3**.

Testing for adduct formation within the mixing time

All absorbance – time curves start at the same level and no absorbance jump in the UV/Vis spectra was observed. This is important to exclude the accumulation of a GH·olefin intermediate in the course of the initiation reaction. As an example this is shown in figure SI-42 for **1(NO$_2$)**. All other complexes behave accordingly.

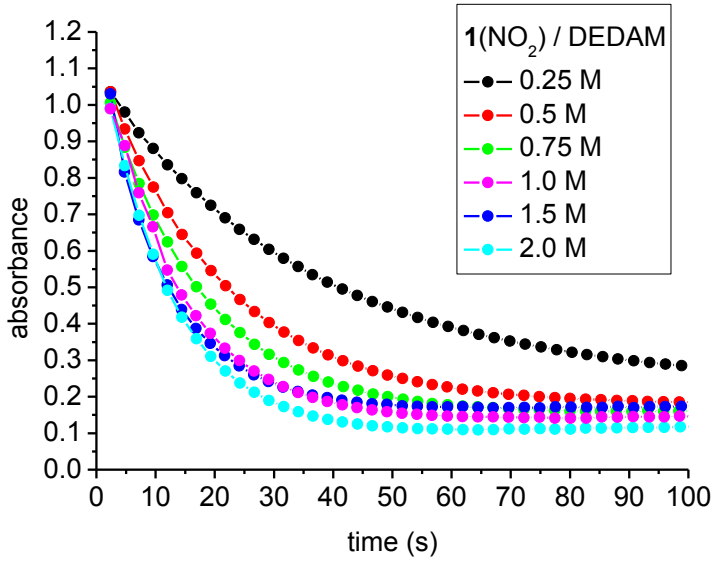

Figure SI-42. Absorbance – time curves at 419 nm from the reaction of **1(NO$_2$)** with different DEDAM concentrations (0.25 – 2.0 M).

c(DEDAM) [M]	1(H)	1(F)	1(NO_2)	1(OiPr)	1(NEt_2)	2(F)	2(NO_2)	2(OiPr)	2(NEt_2)	2(Me)	3(H)	3(NO_2)
0.01	1.17E+01	7.19E+01	0.00113	6.31E-01	9.76E-01	4.57E+01	4.87E+01	2.36E+01	7.71E+00	7.52E+00	4.39E+01	0.00589
0.025	2.53E+01	0.00112	0.0028	1.13E+01	1.93E+00	8.69E+01	0.00141	4.75E+01	1.94E+00	1.59E+01	0.00139	0.01199
0.05	5.26E+01	0.00202	0.00747	1.57E+01	3.41E+00	0.00148	0.00323	0.00143	3.90E+01	3.36E+01	0.00275	0.02119
0.075	7.41E+01	0.00255	0.01188	3.13E+01	4.74E+00	0.00214	0.00342	9.46E+01	6.47E+01	3.90E+00	0.00451	0.03326
0.1	9.98E+01	0.00322	0.01301	3.72E+01	6.16E+00	0.00327	0.00542	0.00156	7.93E+01	5.27E+01	0.00569	0.04331
0.25	0.00251	0.00841	0.02736	6.45E+01	1.75538E-4[a]	0.00838	0.01231	0.0035	0.00217	0.00133	0.01444	0.1448
0.5	0.00502	0.01564	0.05003	0.00156	2.73E+01	0.01476	0.01961	0.00665	0.00315	0.00277	0.02712	0.22693
0.75	0.00676	0.02178	0.06206	0.00229	4.21057E-4[b]	0.02077	0.02635	0.00921	0.00472	0.00417	0.04134	0.35844
1	0.00867	0.02754	0.07744	0.00313	5.14E+01	0.02547	0.03446	0.01177	0.00622	0.00531	0.05292	0.42393
1.5	0.0119	0.03258	0.08839	0.00449	7.44E+01	0.03047	0.0426	0.01614	0.00875	0.00761	0.07917	0.59518
2	0.01505	0.03893	0.0949	0.00559	9.09E+01	0.03509	0.05266	0.01951	0.0123	0.00986	0.09669	-

Table SI-3. k_{obs} values for DEDAM. Error for measurements is 5%. a) DEDAM concentration was 0.3 M. b) DEDAM concentration was 0.8 M.

Reactions with 1-hexene

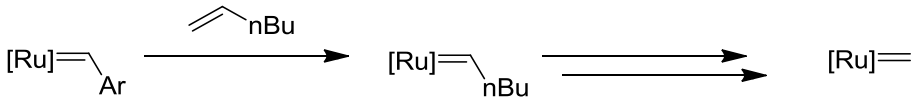

Reactions of 1-hexene with Grubbs-Hoveyda type complexes behave like those of DEDAM and require the same kinetic treatment. As representative examples the UV/Vis traces and absorbance – time curves for **1(H)** with 0.01 M and 2.0 M 1-hexene are shown in figures SI-43 and SI-44. The other complexes and substrate concentrations behave accordingly.

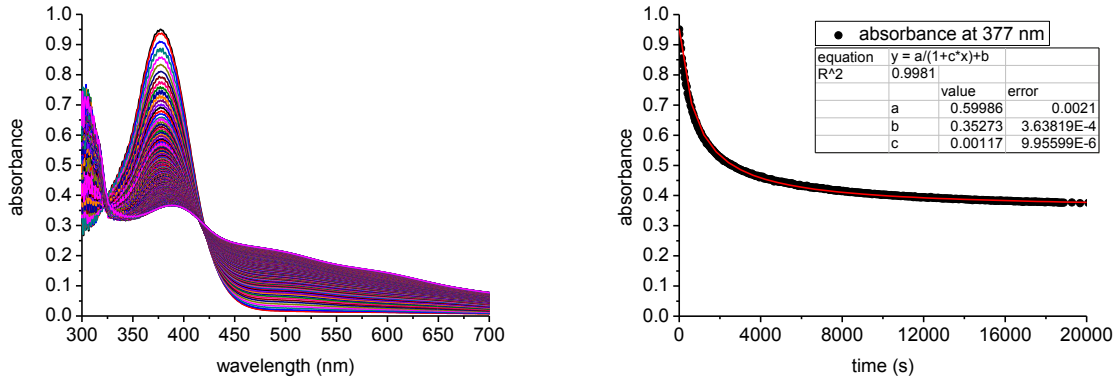

Figure SI-43. Left: UV/Vis traces of **1(H)** ($1.00 \cdot 10^{-4}$ M) with reaction with 1-hexene (0.01 M). Spectra are recorded with Δt = 40 s. Right: Corresponding absorbance – time curves at 377 nm. The data are fitted using ($y = a/(1+c \cdot x) + b$) and ($k_{obs} = c$).

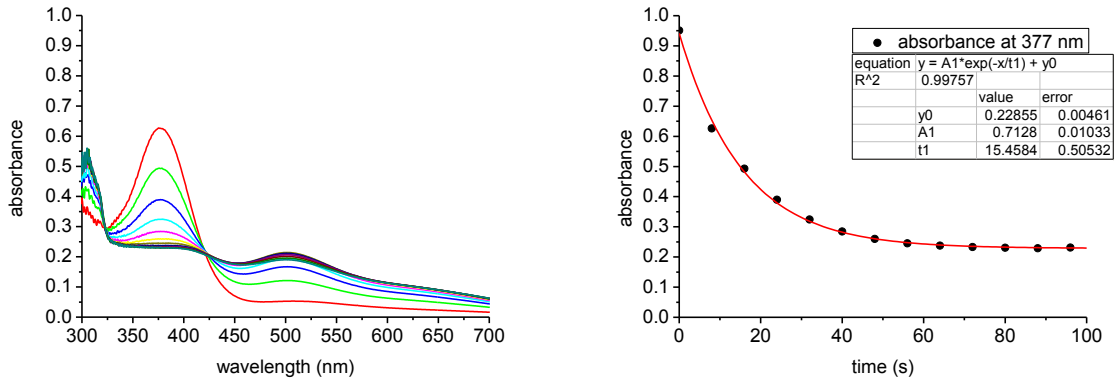

Figure SI-44. Left: UV/Vis traces of **1(H)** ($1.00 \cdot 10^{-4}$ M) with reaction with 1-hexene (2.0 M). Spectra are recorded with Δt = 8 s. Right: Corresponding absorbance – time curves at 377 nm. The data are fitted using ($y = A1 \cdot \exp(-x/t1) + y0$) and ($k_{obs} = 1/t1$).

The k_{obs} vs. [1-hexene] plots are shown in figure SI-45.

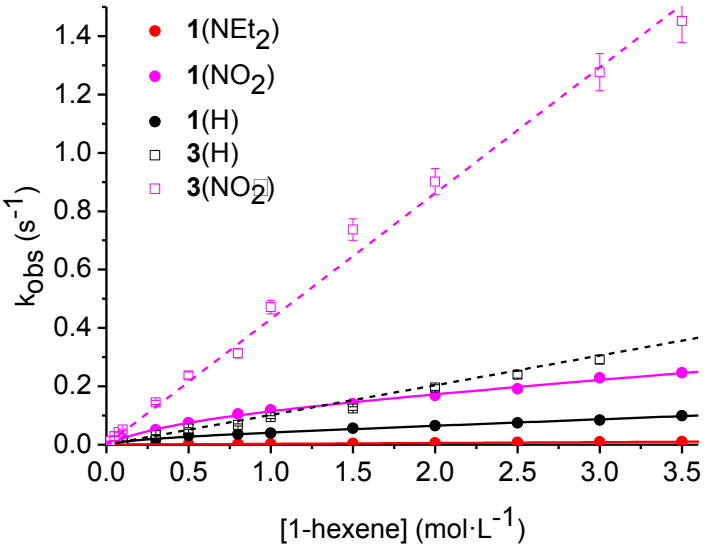

Figure SI-45 k_{obs} vs. [1-hexene] plots. The data are fitted using (y = a·b·x/(1+b·x)+c·x) for complexes **1(H)** and **1(NO₂)** (y = c·x) for complexes **3** and **1(NEt₂)**.

c(1-hexene) [M]	**1(H)**	**1(NO_2)**	**1(NEt_2)**	**3(H)**	**3(NO_2)**
0.01	0.00117	0.00234	2.37787E-5	0.00134	0.00517
0.025	0.00521	0.00791	5.36595E-5	0.0032	0.01195
0.05	0.00484	0.01112	9.54088E-5	0.006	0.02933
0.075	0.00703	0.01592	1.43875E-4	0.00843	0.04287
0.1	0.00889	0.02147	2.19584E-4	0.01144	0.05136
0.3	0.02038	0.05103	0.00106	0.03219	0.14496
0.5	0.03057	0.07563	0.00195	0.05524	0.23713
0.8	0.03622	0.10516	0.00398	0.06787	0.31336
1.0	0.03933	0.11939	0.00242	0.09424	0.47169
1.5	0.05631	0.14085	0.00412	0.1236	0.73754
2.0	0.06469	0.16887	0.00568	0.19558	0.90152
2.5	0.07464	0.19161	0.00741	0.23991	-
3.0	0.08461	0.22908	0.00929	0.29177	1.27647
3.5	0.09894	0.24692	0.0108	-	1.45148

Table SI-4. k_{obs} values for 1-hexene. Error for measurements is 5%.

Reactions with neohexene

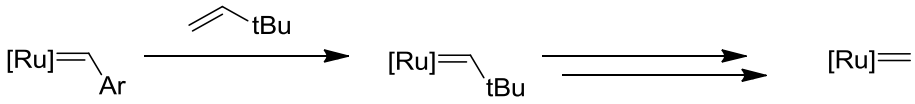

The use of neohexene leads to extremely slow precatalyst initiation, thus only k_{obs} values at very high concentrations (3.0 and 3.5 M) were determined. Fitting with a simple exponential function was not possible. The use of a hyperbolic function is more suitable. Neohexene is a poor initiator, but it is assumed that at high substrate concentrations a significant amount of neohexene is converted into product during the long initiation period. Hence **method 2nd order** was used in the kinetic treatment. As representative examples the UV/Vis traces and absorbance – time curves for **3(H)** and 3.5 M neohexene are shown in figures SI-46. The other complexes and substrate concentrations behave accordingly.

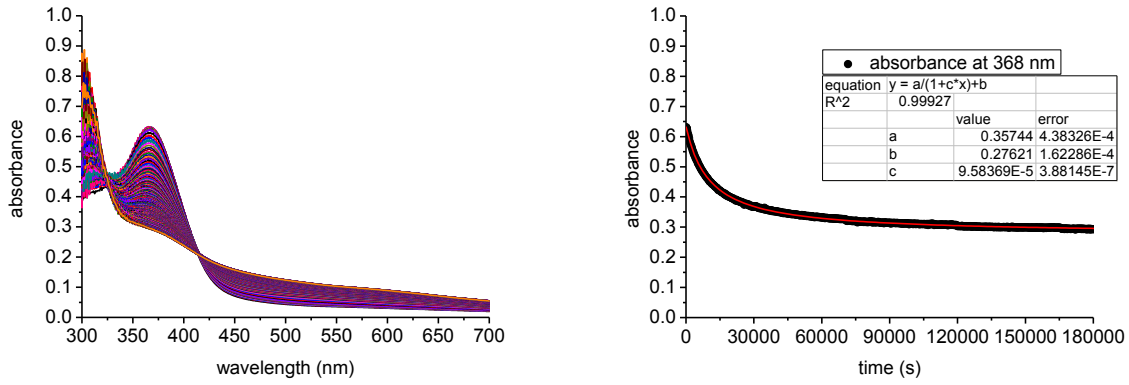

Figure SI-46. Left: UV/Vis traces of **3(H)** ($1.00 \cdot 10^{-4}$ M) with reaction with neohexene (3.5 M). Spectra are recorded with Δt = 40 s. Right: Corresponding absorbance – time curves at 368 nm. The data are fitted using ($y = a/(1+c \cdot x) + b$) and ($k_{obs} = c$).

The k_{obs} vs. [neohexene] plots are shown in figure SI-47.

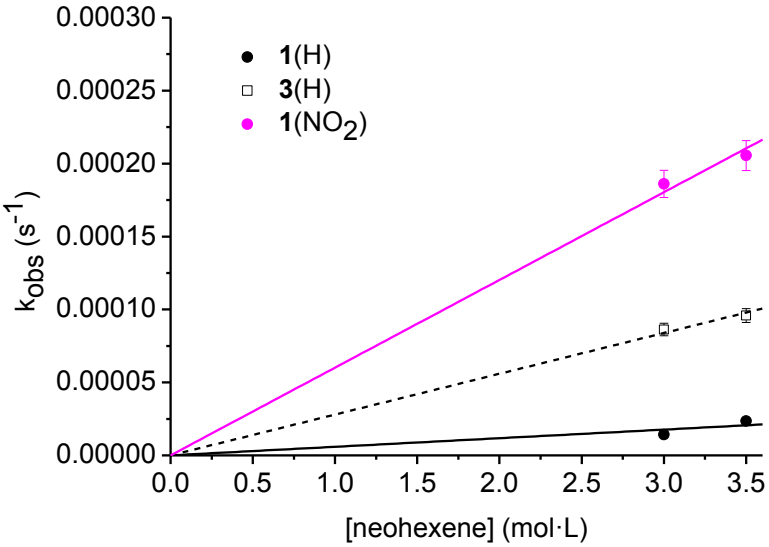

Figure SI-47 k_{obs} vs. [neohexene] plots. The data are fitted using (y = c·x).

c(neohexene) [M]	**1(H)**	**1(NO_2)**	**3(H)**
3.0	1.42183E-5	1.86058E-4	8.62304E-5
3.5	2.35557E-5	2.05515E-4	9.58369E-5

Table SI-5. k_{obs} values for neohexene. Error for measurements is 5%.

Reactions with styrene

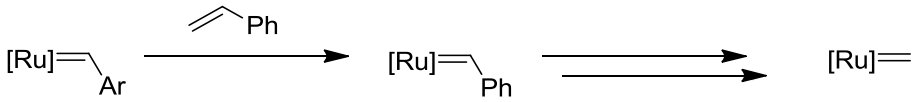

Reactions of styrene with Grubbs-Hoveyda type complexes behave like those of DEDAM and require the same kinetic treatment. As representative examples the UV/Vis traces and absorbance – time curves for **1(H)** with 0.05 M and 1.5 M styrene are shown in figures SI-48 and SI-49. The other complexes and substrate concentrations behave accordingly.

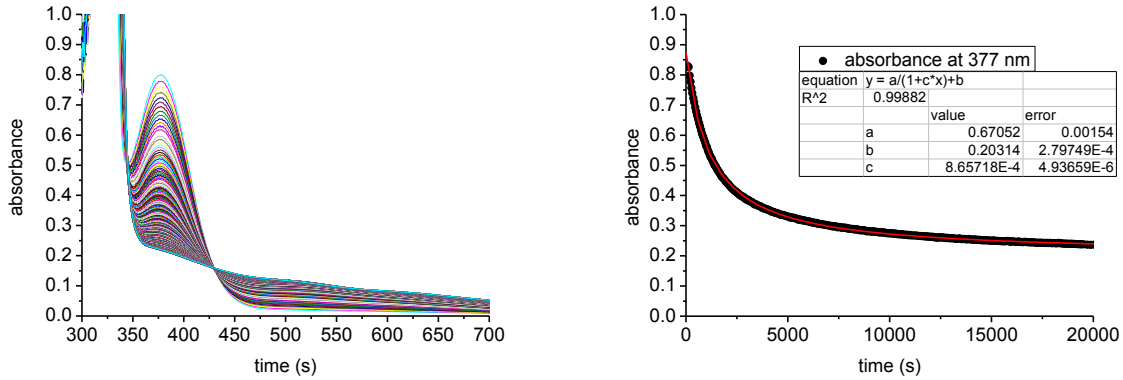

Figure SI-48. Left: UV/Vis traces of **1(H)** ($1.00 \cdot 10^{-4}$ M) with reaction with styrene (0.05 M). Spectra are recorded with Δt = 40 s. Right: Corresponding absorbance – time curves at 377 nm. The data are fitted using ($y = a/(1+c \cdot x) + b$) and ($k_{obs} = c$).

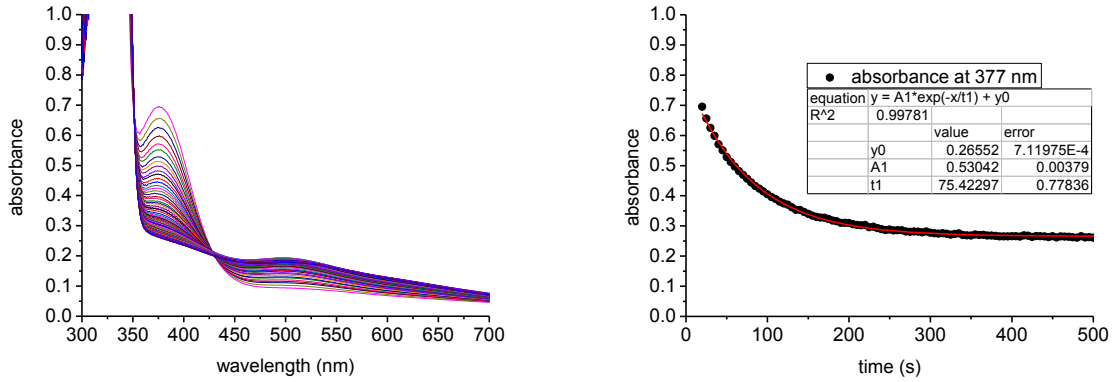

Figure SI-49 Left: UV/Vis traces of **1(H)** ($1.00 \cdot 10^{-4}$ M) with reaction with styrene (1.5 M). Spectra are recorded with Δt = 5 s. Right: Corresponding absorbance – time curves at 377 nm. The data are fitted using ($y = A1 \cdot \exp(-x/t1) + y0$) and ($k_{obs} = 1/t1$).

The k_{obs} vs. [styrene] plots are shown in figure SI-50.

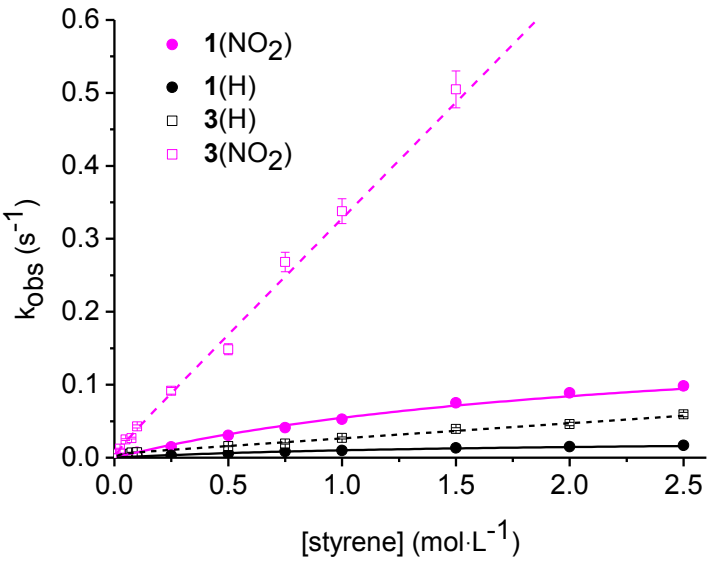

Figure SI-50 k_{obs} vs. [styrene] plots. The data are fitted using (y = a·b·x/(1+b·x)+c·x) for complex **3(H)** and (y = c·x) for complex **3(NO$_2$)** and (y = a·b·x/(1+b·x)) for complexes **1**.

c(styrene) [M]	**1(H)**	**1(NO$_2$)**	**3(H)**	**3(NO$_2$)**
0.01	1.60368E-4	0.00101	0.00256	0.00536
0.025	4.60761E-4	0.00222	0.00414	0.01232
0.05	8.65718E-4	0.00374	0.00527	0.02484
0.075	0.00114	0.00569	0.00689	0.02685
0.1	0.00187	0.00729	0.0074	0.04269
0.25	0.003	0.01481	0.01574	0.09178
0.5	0.00571	0.03045	0.01947	0.14867
0.75	0.00841	0.04118	0.02709	0.26825
1.0	0.00969	0.05283	0.03916	0.33789
1.5	0.01326	0.07509	0.04608	0.50485
2.0	0.01509	0.08869	0.05928	0.65212
2.5	0.0168	0.09844	0.00256	0.78514

Table SI-6. k_{obs} values for styrene. Error for measurements is 5%.

Reactions with PCy_3

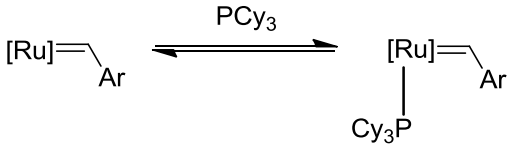

Reactions of PCy_3 with Grubbs-Hoveyda type complexes are simple ligand substitution reactions, which lead to an opening of the chelate ring. However, an equilibrium of the respective complex and its PCy_3 adduct is established. The complexes were reacted with different concentrations of PCy_3 (0.001 to 0.3 M) and the change in UV/ Vis spectra was recorded with time. Since the PCy_3 concentration is not depleted during the reaction **method pseudo 1st order** was applied in the kinetic treatment. Due to a better signal-to-noise ratio the absorbance – time traces were made at the right shoulder of the precatalyst's LMCT band. As representative examples the UV/Vis traces and absorbance – time curves for **1(H)** with 0.1 M and PCy_3 are shown in figure SI-51. The other complexes and substrate concentrations behave accordingly.

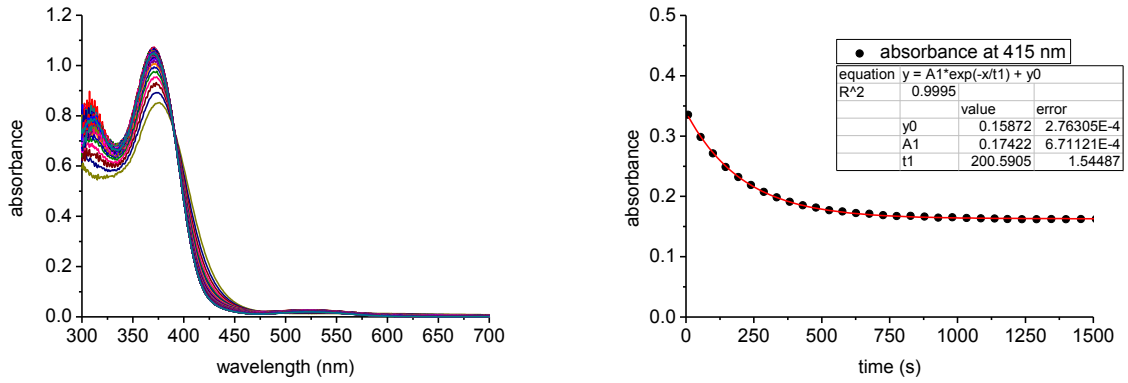

Figure SI-51 Left: UV/Vis traces of **1(H)** (1.00 • 10^{-4} M) with reaction with PCy_3 (0.1 M). Spectra are recorded with Δt = 45 s. Right: Corresponding absorbance – time curves at 377 nm. The data are fitted using (y = A1·exp(-x/t1) + y0) and (k_{obs} = 1/t1).

The k_{obs} vs. [PCy_3] plots are shown in figure SI-52.

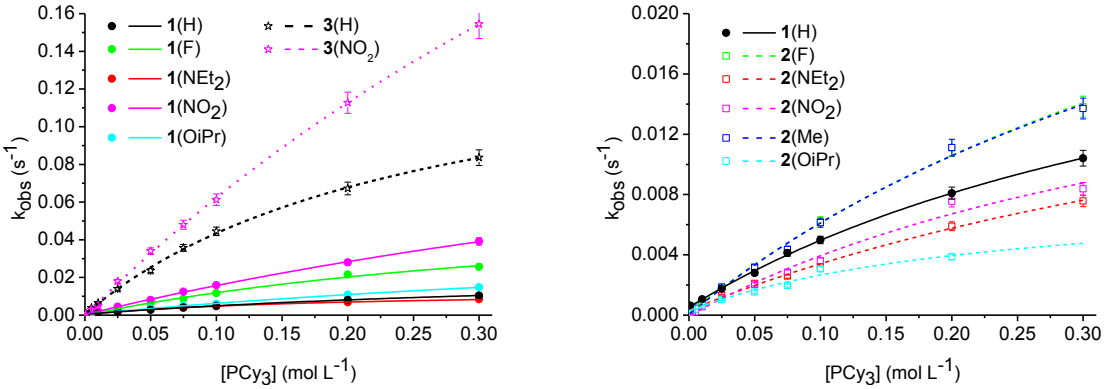

Figure SI-52 Left: k_{obs} vs. [PCy_3] plots for complexes **1** and **3**. Right: k_{obs} vs. [PCy_3] plots for complexes **2**. The data are fitted using (y = a·b·x/(1+b·x)).

c(PCy_3) [M]	**1(H)**	**1(F)**	**1(NO_2)**	**1(OiPr)**	**1(NEt_2)**	**2(F)**	**2(NO_2)**	**2(OiPr)**	**2(NEt_2)**	**2(Me)**	**3(H)**	**3(NO_2)**
0.001	6.29E+01	3.08E+01	4.86E+01	4.30E+01	9.92E-01	2.14E+01	1.25E+01	3.72E+01	2.95E+01	1.13E+01	8.09E+01	8.41E+01
0.005	-	4.16E+01	0.00108	6.63E+01	-	5.99E+01	2.06E+01	4.02E+01	3.47E+01	4.57E+01	0.00383	0.00298
0.01	0.00106	0.00158	0.00213	0.00115	0.00104	9.19E+01	5.49E+00	6.66E+01	7.67E+01	8.75E+01	0.0065	0.00498
0.025	0.00175	0.00346	0.00454	0.0021	0.00198	0.00187	0.00107	0.00103	0.00131	0.00186	0.01391	0.01795
0.05	0.0028	0.00633	0.00806	0.00358	0.00307	0.00319	0.00204	0.00153	0.00211	0.00317	0.02363	0.03396
0.075	0.00412	0.00859	0.01249	0.00514	0.00388	0.00435	0.00285	0.00196	0.00258	0.00436	0.0357	0.04796
0.1	0.00499	0.0117	0.01589	0.00602	0.00469	0.00622	0.00361	0.00307	0.00324	0.00613	0.04448	0.06126
0.2	0.00809	0.0215	0.02801	0.01082	0.0068	0.01109	0.00755	0.00387	0.0059	0.01111	0.06725	0.1127
0.3	0.01041	0.02566	0.03913	0.01482	0.00839	0.01383	0.00838	-	0.00758	0.0137	0.08357	0.15448

Table SI-7. k_{obs} values for PCy_3. Error for measurements is 5%.

Styrene release

The styrene release can be monitored for the Grubbs-Hoveyda complex **1(NO$_2$)** since the UV/Vis absorbance of the free styrene and the precatalyst can be clearly distinguished in this case (see figure SI-46). The decay of the precatalyst's LMCT band at 419 nm and the increase in the styrene band at 350 nm are compared during the initiation reaction with BuVE and DEDAM.

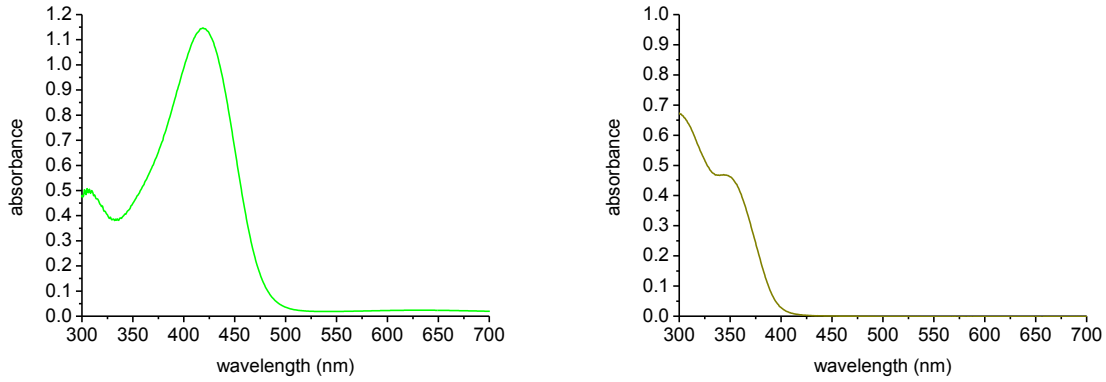

Figure SI-46 Left: UV/Vis trace of **1(NO$_2$)** (1.00 • 10^{-4} M). Right: UV/Vis trace of 2-isopropoxy-4-nitrostyrene (1.00 • 10^{-4} M).

The k_{obs} values obtained for the reaction of **1(NO$_2$)** with BuVE are identical within the error of the experiments. This holds true for both low and high concentrations of olefin (see figures SI-47 and SI-48).

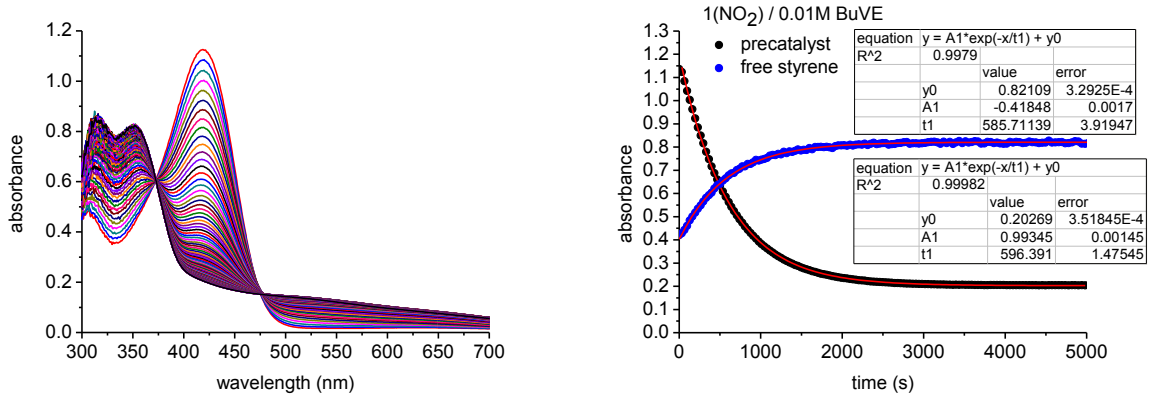

Figure SI-47 Left: UV/Vis traces of **1(NO$_2$)** (1.00 • 10^{-4} M) with reaction with BuVE (0.01 M). Spectra are recorded with Δt = 40 s. Right: Corresponding absorbance – time curves at 350 & 419 nm. The data are fitted using (y = A1·exp(-x/t1) + y0) and (k_{obs} = 1/t1).

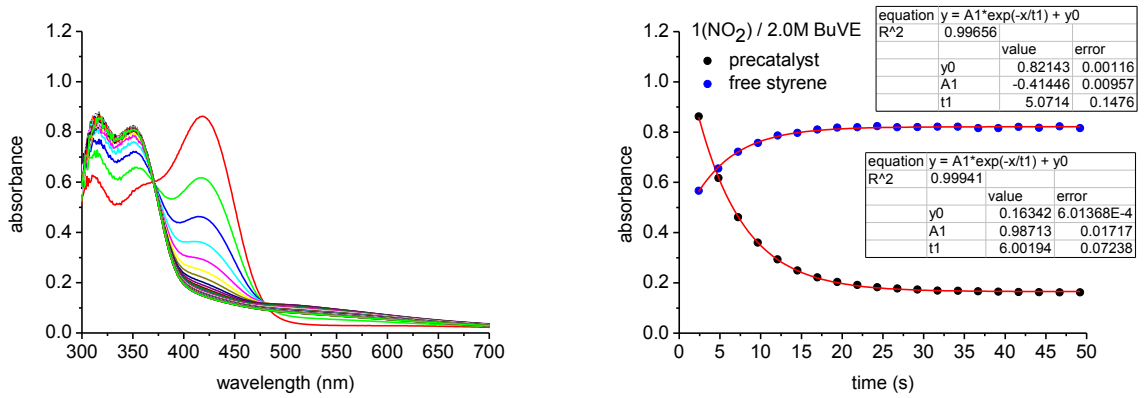

Figure SI-48 Left: UV/Vis traces of **1(NO$_2$)** (1.00 • 10^{-4} M) with reaction with BuVE (2.0 M). Spectra are recorded with Δt = 2 s. Right: Corresponding absorbance – time curves at 350 & 419 nm. The data are fitted using (y = A1·exp(-x/t1) + y0) and (k$_{obs}$ = 1/t1).

Nearly the same behavior is observed at a low temperature of -20 °C (see figure SI-49).

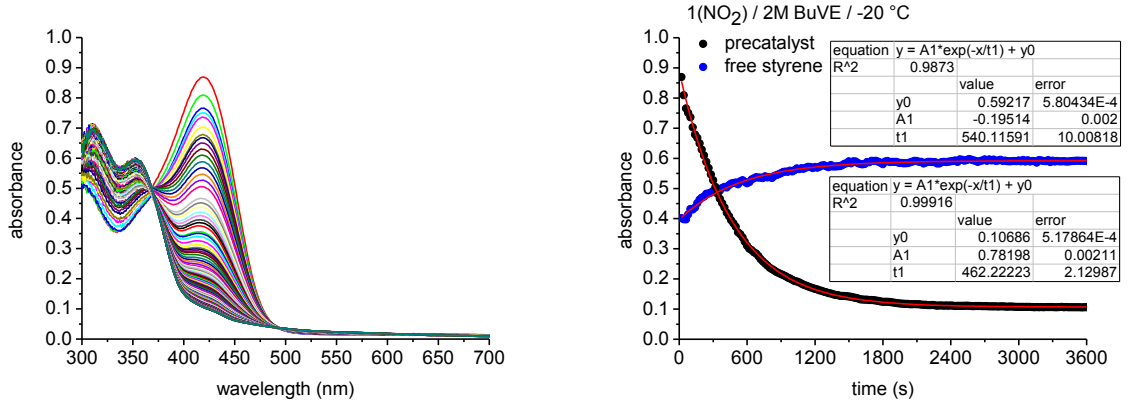

Figure SI-49 Left: UV/Vis traces of **1(NO$_2$)** (1.00 • 10^{-4} M) with reaction with BuVE (2.0 M) at -20 °C. Spectra are recorded with Δt = 20 s. Right: Corresponding absorbance – time curves at 350 & 419 nm. The data are fitted using (y = A1·exp(-x/t1) + y0) and (k$_{obs}$ = 1/t1).

The k$_{obs}$ vs. [DEDAM] plots derived from the reaction of **1(NO$_2$)** with DEDAM give similar rate constants for the decay of the precatalyst and the increase of the styrene ligand (see figure SI-50).

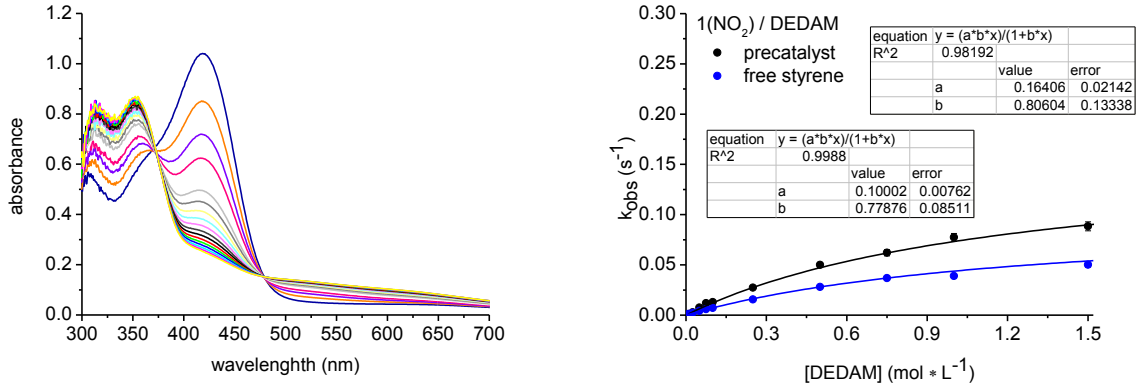

Figure SI-50 Left: UV/Vis traces of **1(NO$_2$)** (1.00 • 10^{-4} M) with reaction with DEDAM (0.05 M). Spectra are recorded with Δt = 40 s. Right: k_{obs} vs. [DEDAM] plots. The data are fitted using (y = a·b·x/(1+b·x)).

Eyring and Arrhenius plots

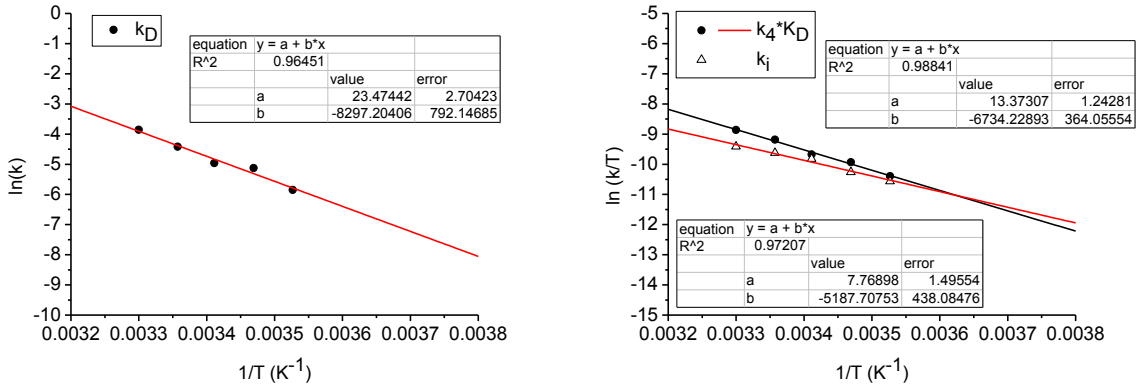

Figure SI-51 Left: Arrhenius plot of **1(H)** with reaction with BuVE for k_D. Right: Eyring plot of **1(H)** with reaction with BuVE for $k_4 \cdot K_D$ and k_i.

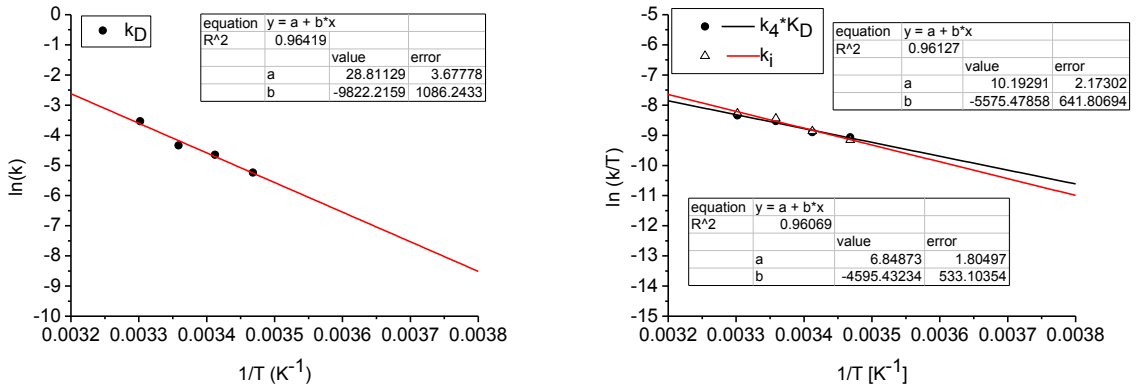

Figure SI-52 Left: Arrhenius plot of **1(NO$_2$)** with reaction with BuVE for k_D. Right: Eyring plot of **1(NO$_2$)** with reaction with BuVE for $k_4 \cdot K_D$ and k_i.

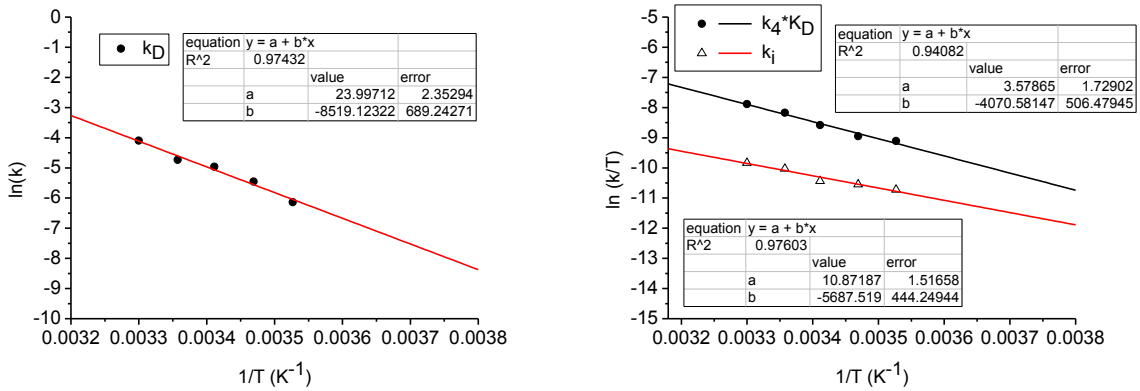

Figure SI-53 Left: Arrhenius plot of **1(NEt$_2$)** with reaction with BuVE for k_D. Right: Eyring plot of **1(NEt$_2$)** with reaction with BuVE for $k_4 \cdot K_D$ and k_i.

Hammett plots

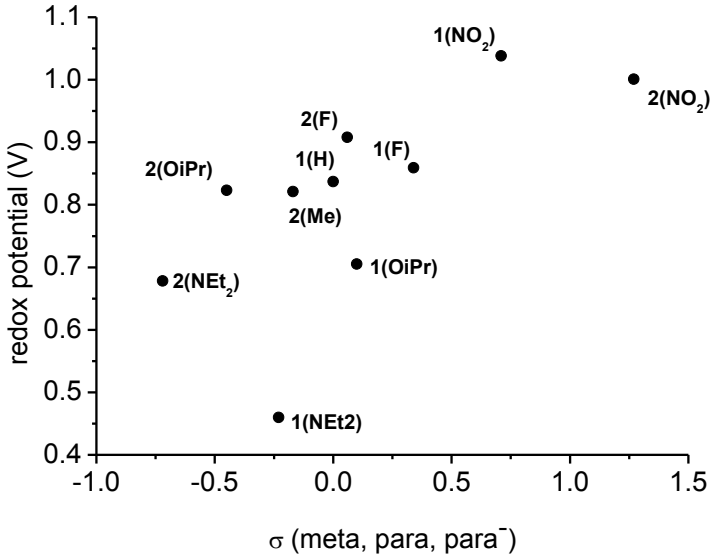

Figure SI-54 Plot of redox potentials vs. Hammett σ-parameter of the R4 (meta) and R5 (para, para$^-$) group in complexes **1** and **2** relative to the isopropoxy group.

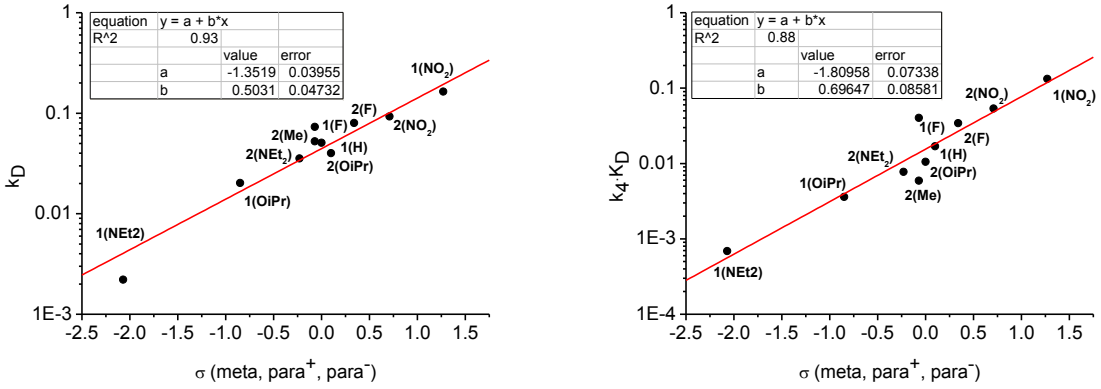

Figure SI-55 Left: Plot of k_D vs. Hammett σ-parameter of the R4 (para$^+$, para$^-$) and R5 (meta) group in complexes **1** and **2** relative to the benzylidene carbon derived from the reaction with DEDAM. Right: Plot of $k_4 \cdot K_D$ vs. Hammett σ-parameter of the R4 (para$^+$, para$^-$) and R5 (meta) group in complexes **1** and **2** relative to the benzylidene carbon derived from the reaction with DEDAM.

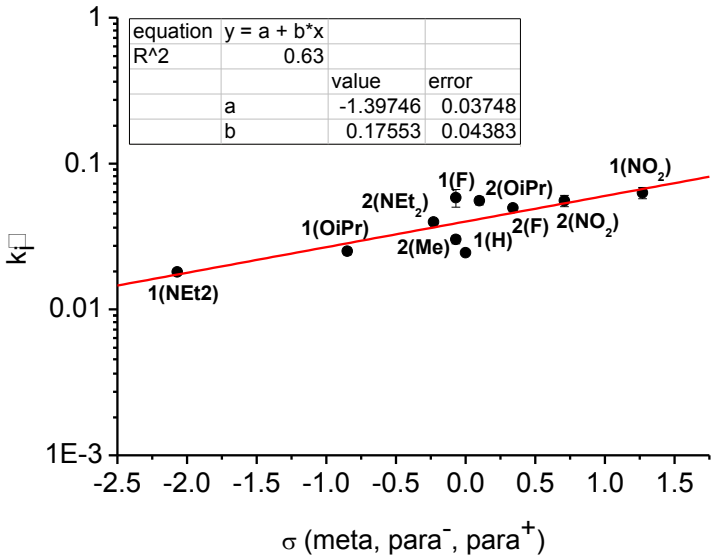

Figure SI-56 Plot of k_i vs. Hammett σ-parameter of the R4 (para$^+$, para$^-$) and R5 (meta) group in complexes **1** and **2** relative to the benzylidene carbon derived from the reaction with BuVE.

References

(1) Schmidt, V. A.; Alexanian, E. J. *Angew. Chem., Int. Ed.* **2010**, *49*, 4491-4494.

(2) Zaja, M.; Connon, S. J.; Dunne, A. M.; Rivard, M.; Buschmann, N.; Jiricek, J.; Blechert, S. *Tetrahedron* **2003**, *59*, 6545-6558.

(3) Michrowska, A.; Bujok, R.; Harutyunyan, S.; Sashuk, V.; Dolgonos, G.; Grela, K. *J. Am. Chem. Soc.* **2004**, *126*, 9318-9325.

(4) Method for preparation of ruthenium-based metathesis catalyst with chelating alkylidene ligand, Doppiu, A.; Winde, R.; Wörner, E.; Rivas-Nass, A.; Slugovc, C.; Lexer, C. Patent WO 2010/127829.

(5) Barbasiewicz, M.; Bieniek, M.; Michrowska, A.; Szadkowska, A.; Makal, A.; Wozniak, K.; Grela, K. *Adv. Synt. Cat.* **2007**, *349*, 193-203.

(6) Vorfalt, T.; Wannowius, K.-J.; Thiel, V. Plenio, H. *Chem. Eur. J.* **2010**, *16*, 12312-12315.

(7) Henley, R. V.; Turner, E. E. *J. Chem. Soc.* **1930**, 928-940.